universität wien

MASTERARBEIT

Titel der Masterarbeit

„Calculating forces in the random phase approximation“

verfasst von

BBSc. Benjamin Ramberger

angestrebter akademischer Grad

Master of Science (MSc.)

Wien, 2015

Studienkennzahl lt. Studienblatt:	A 066 876
Studienrichtung lt. Studienblatt:	Masterstudium Physik
Betreut von:	Univ.-Prof. Dipl.-Ing. Dr. Georg Kresse

Acknowledgements

I want to express my sincere thanks to my supervisor Georg Kresse for his great support throughout this thesis. He was very encouraging and guided me into the right direction whenever I needed it. It was an honour to work with such a keen thinker and I really appreciated his direct and open attitude. I also want to thank Felix Hummel who answered so many of my questions and shared his knowledge with me. His bright personality and his enthusiasm in our discussions were also an inspiration for me. Another colleague to whom I am very much obliged is Andreas Grüneis, whose profound knowledge and patience is admirable. Merzuk Kaltak was also very helpful. It kind of felt like his pioneering work was the driving force for my own project and I am very grateful for that. At this point I want to add that I am very thankful that Doris Hecht-Aichholzer and Katharina Simma helped me a lot to introduce myself to the group. Finally I want to thank all other colleagues in the Computational Materials Physic Group that they welcomed me so nicely. It was a pleasure to work here and it makes me happy that I can frankly say that colleagues became also friends in the past few months.

Of course I also want to thank all the people that accompanied me in my private life. First and foremost I am very grateful that my parents, Maria Ramberger and Rudolf Ramberger, always supported me and gave me the opportunity to focus entirely on my studies. The discussions on physical problems with my father boosted my excitement about the subject, while the caring personality of my mother gave me the necessary confidence. My brother, Severin Ramberger, also deserves to be mentioned here explicitly, since his vivid approach to science was definitely very important for my professional development. I also want to thank Catalina Royuela, who inspired me in so many ways. I drew an incredible amount of motivation from my relationship with her. Last but not least I want to thank all my beloved friends. They always keep my life in balance and grant me the energy to sustain my capabilities.

Abstract

Recently there has been a lot of progress in the development of computer simulations employing the Random Phase Approximation (RPA) so that RPA-correlation energies became accessible for large systems. However, there is not yet an efficient way to calculate forces in the RPA within the current framework. Since the calculation of forces is crucial for the simulation of elastic and vibrational properties as well as for structure relaxations, this is a promising area for further investigation. In this work, analytical expressions that might allow an efficient numerical calculation of forces within the RPA are established. This was done using the Green's function formalism and finally the results were also translated into Feynman diagrams. Additionally in the first part of this thesis, a state of the art algorithm for the calculation of the RPA-correlation energy was used to evaluate the binding energy of some complexes from the S22-test set.

Zusammenfassung

Kürzlich wurden große Fortschritte bei der Entwicklung von Computersimulationen erzielt, welche auf der so genannten Random-Phase-Approximation (RPA) beruhen. Dadurch wurde es möglich, die RPA-Korrelationsenergien auch für große Systeme zu berechnen. Allerdings gibt es mit den gängigen Methoden bislang keinen effizienten Weg zur Kräfteberechnung in der RPA. Da sich die Berechnung von Kräften als unverzichtbar für die Simulation von elastischen- und Schwingungseigenschaften sowie für Strukturrelaxationen darstellt, scheint es sich bei diesem Thema um ein viel versprechendes Forschungsgebiet zu handeln. Im Zuge dieser Arbeit wurden analytische Ausdrücke entwickelt, welche die Basis legen um in Zukunft Kräfte in der RPA mittels Computersimulationen effizient zu berechnen. Dies wurde unter Verwendung des Greensfunktionenformalismus erreicht wobei zum Schluss die Ergebnisse zusätzlich Feynman-diagrammatisch dargestellt wurden. Zusätzlich wurden im ersten Teil der Arbeit RPA-Bindungsenergien von bimolekularen Komplexen des S-22 Testsatzes berechnet. Dies geschah mittels eines Algorithmus der in diesem Gebiet dem neuesten Stand der Technik entspricht.

Contents

1 Introduction

The research and exploration of new materials has become very important in many different areas. The ever growing requirements for different components used in the electronic industry or the demand for robust, heat resistant materials in the development of fusion reactors are just two prominent examples of an endless list where technological progress is limited by the availability of suitable materials. Besides the development of materials with outstanding properties, it is worthwhile looking for replacing existing materials by new ones, which are more easily producible.
In modern materials science, many materials can be modelled by computer simulations based on theoretical descriptions made by solid state physics. In comparison to conventional laboratory techniques, this brings the advantage that a large number of materials can be screened in a rather short period of time. Although the fundamental theories to describe most common materials are already well developed, not all of them can be implemented efficiently for computation. The crucial property of an algorithm which is supposed to determine properties of bulk materials is its scaling with system size. If the scaling is too unfavourable, the computational time is rapidly increasing for large systems. Therefore not all models that theoretically describe the behaviour of a system are suitable for computational methods. In many cases, certain approximations have to be made in order to conduct calculations efficiently. However, as soon as approximations are applied, errors occur. These errors might be sufficiently small for some materials to be well described, but might not be neglected for others. In the past, density functional theory (DFT) was exploited extensively to calculate a vast variety of materials. The two most common approximations that were made to actually compute different problems are the local density approximation (LDA) and the generalized gradient approximation (GGA). These methods will probably be continuously used in the near future, as they yield good results for many materials and properties, but there are also major drawbacks to be overcome. Today many researchers focus on developing new less approximate methods, in order to describe strongly correlated materials and to produce results closer to the experimental values. One method that has been increasingly investigated recently is the random phase approximation (RPA). The RPA may be applied to problems that cannot be solved correctly with LDA or GGA, and due to recent progress it is expected to become a feasible method with a large field of application in the near future. For example, in a recent publication [1], an efficient method to calculate the RPA correlation energy was presented, which scales only cubically in system size. Still, it is not yet possible to simulate molecular dynamics efficiently within the RPA.
The ability to conduct relaxations is crucial for a method. Otherwise, one has to rely

on other methods to obtain the geometry of the atoms under investigation and therefore cannot simulate systems entirely within the framework of the desired method. In relaxation calculations, as well as in molecular dynamics simulations, usually the forces acting on the different atoms are calculated and the atoms are moved in the direction of the force. Therefore it is very important to have an efficient way of calculating the forces within the RPA. Different approaches have already been used to calculate these forces, for example by constructing a Lagrangian for the RPA using the resolution-of-identity and imaginary frequency integration [2]. In this thesis, a different approach to calculate the forces within the RPA is shown. The main idea is to calculate the forces variationally from the Green's functions. The gradient of the RPA correlation energy with respect to the atomic positions is calculated via the variation of the independent particle polarizability which is related to the imaginary time Green's function by Hedin's equation. Hence, the forces in the RPA are in principle related to the variation of the Green's function with respect to atomic positions. This approach seems promising as the imaginary time Green's functions are already accessible with cubic scaling in system size [1].

In the first section of this thesis, the theory of Kohn Sham DFT is reviewed. The focus is to give the reader a quick overview over this method and establish the connection to the more advanced RPA. This section closes with a summary over the limitations of DFT. In the next section, the RPA is motivated from linear response theory. It is shown that the polarizability plays an important role in this formulation and how the independent particle polarizability χ^0 is connected to DFT. To obtain the equation for the RPA correlation energy $E_\mathrm{c}^\mathrm{RPA}$, the adiabatic connection dissipation-fluctuation theorem (ACFDT) is used. It is shown that the RPA correlation energy can be calculated from the independent particle polarizability χ^0 only, which in turn can be expressed in terms of the Kohn-Sham orbitals.

In section 4, simulations that were carried out using the method described in [1] are discussed, in order to gain insight into state of the art applications of the theoretical framework discussed before. In particular, the binding energies of some bimolecular complexes from the S-22 test set were evaluated. Additionally simulations with the *DFT-D2 method of Grimme* [3] were carried out and compared with the RPA results. The results were also compared with literature values from *Zhu* and coworkers [4].

After that, the Green's function formalism is presented briefly. In the following it is discussed that for a small perturbation of the Hamiltonian δV, the Green's function can be approximated by the first order term of the Dyson equation. This is used to express the density operator in terms of the Green's function and it turns out that the result is in agreement with standard first order perturbation theory.

With this framework, the variations $\frac{\delta E}{\delta V}$ of the different energy contributions with respect to the KS-potential are derived. This was done for the Hartree energy (E_{H}), the exchange energy (E_{x}) and the RPA-correlation energy ($E_{\mathrm{c}}^{\mathrm{RPA}}$) as well as for the kinetic energy E_{kin} and the electrostatic energy due to the positively charged cores E_{ext}. The results are related to the forces by a chain rule for functional derivatives, that considers the derivative of the KS-potential with respect to atomic positions $\nabla_{\boldsymbol{R}} V$.

Finally, the results for the energy variations were translated into Feynman diagrams in order to condense them into a more compact form and to be able to use them in the more intuitive diagrammatic framework.

2 Density functional theory

The origin of density functional theory reaches back to the 1920's, when the Thomas-Fermi method was developed. The Thomas-Fermi model is a semi-classical approach, trying to describe the electron density in atoms. In contrast to the typical quantum mechanical wave function formalism, the Thomas-Fermi model is based on the electron density $n(\boldsymbol{r})$. It tries to describe the electronic behaviour in an external potential by means of statistical methods assuming the electron density is describing the state completely. One idea was that the electron density, although not uniformly distributed, is approximated by a locally uniform distribution. Despite the appealing intuitive approach, the Thomas-Fermi model lacked the ability to describe realistic systems correctly or even yield bound atoms. However, the method was developed further including approximate exchange interactions (Slater Xα method) and was used to roughly describe inhomogeneous systems like atoms, due to its simplicity [5].

2.1 The Hohenberg-Kohn theorems

In 1964 Hohenberg and Kohn published a paper on the inhomogeneous electron gas [5], where they proved that for an interacting electron gas in an external potential $v(\boldsymbol{r})$, there exists a universal energy functional of the density, $F[n(\boldsymbol{r})]$, which yields the correct ground state energy E_0 by minimizing the total energy $E[n(\boldsymbol{r})]$ with respect to the density:

$$E_0 = \min_{n(\boldsymbol{r})}\{E[n(\boldsymbol{r})]\} = \min_{n(\boldsymbol{r})}\{\int v(\boldsymbol{r})n(\boldsymbol{r}) + F[n(\boldsymbol{r})]\}. \tag{1}$$

The essential proofs for this theorem are presented in equation (2) to (16), following basically the original work of Hohenberg and Kohn. A general Hamiltonian for a inhomogeneous electron gas in an external potential $v(r)$ can be written as

$$H = T + V + U \tag{2}$$

where T denotes the kinetic energy operator, V the operator of the external potential, and U the operator of Coulomb interaction between the interacting electrons. In second quantization these operators are written in terms of the field operators $\psi(\boldsymbol{r})$ and $\psi^\dagger(\boldsymbol{r})$

as follows:

$$T \equiv \frac{1}{2}\int \nabla\psi^\dagger(\boldsymbol{r})\nabla\psi(\boldsymbol{r})d\boldsymbol{r} \tag{3}$$

$$V \equiv \int v(\boldsymbol{r})\psi^\dagger(\boldsymbol{r})\psi(\boldsymbol{r})d\boldsymbol{r} \tag{4}$$

$$U \equiv \frac{1}{2}\int \frac{1}{|\boldsymbol{r}-\boldsymbol{r}'|}\psi^\dagger(\boldsymbol{r})\psi(\boldsymbol{r}')\psi^\dagger(\boldsymbol{r}')\psi(\boldsymbol{r})d\boldsymbol{r}d\boldsymbol{r}'. \tag{5}$$

The electronic density of the ground state Ψ is given by

$$n(\boldsymbol{r}) \equiv \langle\Psi|\psi^\dagger(\boldsymbol{r})\psi(r)|\Psi\rangle\,. \tag{6}$$

Assuming the ground state Ψ is non-degenerate, $n(\boldsymbol{r})$ is a unique functional of the external potential $v(\boldsymbol{r})$ as the ground state Ψ is uniquely determined by $v(\boldsymbol{r})$. In the following it is shown that also for a given density $n(\boldsymbol{r})$ the potential $v(\boldsymbol{r})$ is a unique functional of the density. In other words, there is an bijective mapping between densities and potentials. The proof proceeds by *reductio ad absurdum*. Assume there are two potentials $v(\boldsymbol{r})$ and $v'(\boldsymbol{r})$ that give rise to the same density $n(\boldsymbol{r})$. The Hamiltonian associated with the external potential $v'(\boldsymbol{r})$ is denoted by H' and Ψ' shall be the corresponding ground state. Unless in the trivial case where $v'(\boldsymbol{r}) - v(\boldsymbol{r}) = const$, the solutions to the two Schrödinger equations $H\,|\Psi\rangle = E\,|\Psi\rangle$ and $H'\,|\Psi'\rangle = E'\,|\Psi'\rangle$ will be different. Since we are assuming non degenerate ground states and because the ground state minimizes the energy, i.e. the expectation value of the Hamiltonian, the following inequality holds

$$E' = \langle\Psi'|H'|\Psi'\rangle < \langle\Psi|H'|\Psi\rangle = \langle\Psi|H - V + V'|\Psi\rangle = E + \int[v'(\boldsymbol{r}) - v(\boldsymbol{r})]n(\boldsymbol{r})d\boldsymbol{r}. \tag{7}$$

By interchanging the unprimed and primed quantities a similar inequality is found

$$E = \langle\Psi|H|\Psi\rangle < \langle\Psi'|H|\Psi'\rangle = \langle\Psi'|H' - V' + V|\Psi'\rangle = E' + \int[v(\boldsymbol{r}) - v'(\boldsymbol{r})]n(\boldsymbol{r})d\boldsymbol{r}. \tag{8}$$

Adding these together yields the inconsistency

$$E' + E < E + E'. \tag{9}$$

Thus for a given ground state density $n(\boldsymbol{r})$, there is an (up to a constant) unique potential $v(\boldsymbol{r})$ which gives rise to $n(\boldsymbol{r})$. As the Hamiltonian H is fixed by $v(\boldsymbol{r})$, the many-particle ground state Ψ is a unique functional of the density. Summarized, for

nondegenerate ground states, $n(\boldsymbol{r})$ is a unique functional of the potential $v(\boldsymbol{r})$ and vice versa.

$$v(\boldsymbol{r}) \Leftrightarrow n(\boldsymbol{r}). \tag{10}$$

Since the ground state wave functionΨ is a functional of the density $n(\boldsymbol{r})$, the kinetic energy T and the interaction energy U are also determined by $n(\boldsymbol{r})$. One can formally define a functional, which gives the correct kinetic and interaction energy for a given $n(\boldsymbol{r})$,

$$F[n(\boldsymbol{r})] \equiv \langle \Psi | T + U | \Psi \rangle \,. \tag{11}$$

For the correct $n(\boldsymbol{r})$ to a given potential $v(\boldsymbol{r})$, from now on in this section denoted as $n_v(\boldsymbol{r})$, the energy functional

$$E_v[n] \equiv \int v(\boldsymbol{r}) n(\boldsymbol{r}) d\boldsymbol{r} + F[n] \tag{12}$$

equals the ground state energy E_{GS}

$$E_v[n_v] = \int v(\boldsymbol{r}) n_v(\boldsymbol{r}) d\boldsymbol{r} + F[n_v] = \langle \Psi_v | V | \Psi_v \rangle + \langle \Psi_v | T + U | \Psi_v \rangle = E_{\mathrm{GS}}. \tag{13}$$

Furthermore $E_v[n]$ is minimal for n_v, if the admissible functions $n(\boldsymbol{r})$ are restricted such that they give the correct number of particles, i.e.

$$\int n(\boldsymbol{r}) d\boldsymbol{r} = \int n_v(\boldsymbol{r}) d\boldsymbol{r} = N. \tag{14}$$

This follows from the fact that the energy of an N-particle system assumes its minimum for the ground state wave function Ψ_v, compared with all N-particle states Ψ' with arbitrary variations relative to Ψ_v:

$$E_v = \langle \Psi_v | V + T + U | \Psi_v \rangle < \langle \Psi' | V + T + U | \Psi' \rangle \,. \tag{15}$$

Expressed in terms of the energy functional $E_v[n]$ this yields

$$E_v[n'] = \int v(\boldsymbol{r}) n'(\boldsymbol{r}) d\boldsymbol{r} + F[n'] = \langle \Psi' | V + T + U | \Psi' \rangle > E_v. \tag{16}$$

Hence the functional $E_v[n]$ assumes its minimum for n_v and the ground state for a given external potential $v(\boldsymbol{r})$ can be found formally by minimizing the energy functional $E_v[n]$ under the constraint of the correct particle number. However the functional $F[n]$ is not known and one challenging part of density functional theory is to find good approximations for it.

2.2 The Kohn-Sham system of non-interacting electrons

One famous approach to find an approximation for the energy functional in the context of DFT is found in the work of Kohn and Sham from 1965 [6]. The basic idea of this approach is to find an effective potential, which includes the contribution of electron-electron interactions, so that the electrons can be treated as non-interacting particles under the influence of that effective potential. According to the Hohenberg-Kohn theorems, the total energy of a non-uniform electron gas in an static external potential $v(\boldsymbol{r})$ can be written as

$$E = \underbrace{\int v(\boldsymbol{r})n(\boldsymbol{r})d\boldsymbol{r}}_{E_{\text{ext}}} + \underbrace{\frac{1}{2}\int \frac{n(\boldsymbol{r})n(\boldsymbol{r}')}{|\boldsymbol{r}-\boldsymbol{r}'|}d\boldsymbol{r}}_{E_{\text{H}}[n]} + G[n]. \tag{17}$$

Comparing this with equation (12), the classical Coulomb interaction of the electrons, which is referred to as Hartree term $E_{\text{H}}[n]$, is written explicitly, so that the functional $G[n]$ is related with $F[n]$ through

$$G[n] \equiv F[n] - \frac{1}{2}\int \frac{n(\boldsymbol{r})n(\boldsymbol{r}')}{|\boldsymbol{r}-\boldsymbol{r}'|}d\boldsymbol{r}. \tag{18}$$

The Hartree term E_{H} can be interpreted as the classical electrostatic energy of the electrons, due to their own mean field. The energy functional $G[n]$ itself is written as

$$G[n] = T_s[n] + E_{\text{xc}}[n], \tag{19}$$

where $T_s[n]$ is the kinetic energy of a system of non-interacting electrons, which is in analogy to the Hohenberg-Kohn theorems, a unique functional of the electron density. $E_{\text{xc}}[n]$ is a functional that includes all contributions to the energy that arise from exchange and correlation effects, or in other words, all effects that cannot be explained classically. For an arbitrary $n(\boldsymbol{r})$, $E_{\text{xc}}[n]$ cannot be written in a simple exact expression. Though, in the limiting case of slowly varying densities, the so called local density approximation (LDA) offers a simple method to obtain remarkably accurate results. In the LDA the exchange and correlation energy E_{xc} is approximated in the following way

$$E_{\text{xc}} \approx E_{\text{xc}}^{\text{LDA}} = \int n(\boldsymbol{r})\epsilon_{\text{xc}}^{\text{LDA}}(n(r))d\boldsymbol{r}, \tag{20}$$

where $\epsilon_{\text{xc}}^{\text{LDA}}(n)$ is the local exchange correlation energy per particle. In other words, it is assumed that the exchange-correlation energy can be approximated by locally replacing the real exchange-correlation energy density with an approximate form that depends on the density only. In the following, $\epsilon_{\text{xc}}^{\text{LDA}}(n)$ is used synonymous for the exchange and

correlation energy per particle of the uniform electron gas with density n, as this is the most common approximation. The uniform electron gas is a theoretical model which considers the thermodynamic limit at constant density $n = N/V = const.$ of a system of N interacting electrons placed inside a volume V along with a positive compensation charge. That way the Hartree energy cancels against the potential energy due to the positive background charge. Hence, the only contributions to the energy are the kinetic, exchange and correlation energy. This approach was very successful and is still used extensively. From the variational property of the energy functional, see equation (1), one gets from equation (17) the variational equation

$$\int \delta n(r) \underbrace{\left(v(\boldsymbol{r}) + \int \frac{n(\boldsymbol{r}')}{|\boldsymbol{r} - \boldsymbol{r}'|} d\boldsymbol{r}' + \mu_{\mathrm{xc}}(n(\boldsymbol{r})) \right)}_{v_{\mathrm{eff}}^{\mathrm{KS}}} + \frac{\delta T_s[n]}{\delta n(\boldsymbol{r})} d\boldsymbol{r} = 0. \tag{21}$$

The quantity $\mu_{\mathrm{xc}}(n)$ in the local density approximation is given by

$$\mu_{\mathrm{xc}}^{\mathrm{LDA}}(n) = \frac{d(n\epsilon_{\mathrm{xc}}^{\mathrm{LDA}}(n))}{dn} \tag{22}$$

whereas in a more general definition, it would be the variational derivative of E_{xc} with respect to the density,

$$\mu_{\mathrm{xc}}[n](\boldsymbol{r}) = \frac{\delta E_{\mathrm{xc}}[n]}{\delta n(\boldsymbol{r})}. \tag{23}$$

According to the theory of Hohenberg and Kohn, one may interpret equation (21) as the variational equation that stems from a Hamiltonian of the form

$$H^{\mathrm{KS}} = V_{\mathrm{eff}}^{\mathrm{KS}} + T = \int v_{\mathrm{eff}}^{\mathrm{KS}}(\boldsymbol{r}) \psi^*(\boldsymbol{r}) \psi(\boldsymbol{r}) d\boldsymbol{r} - \frac{1}{2} \int \psi^*(\boldsymbol{r}) \Delta \psi(\boldsymbol{r}) d\boldsymbol{r}, \tag{24}$$

which describes a system of non interacting particles moving in the external potential $v_{\mathrm{eff}}^{\mathrm{KS}}(\boldsymbol{r})$. Now obviously the fermionic N-particle ground state Ψ of a system of N non-interacting electrons with the Hamiltonian H^{KS} is obtained by filling up the N lowest one-particle eigenstates ϕ_i^{KS} of the one particle Schrödinger equation

$$H^{\mathrm{KS}} |\phi_m^{\mathrm{KS}}\rangle = \epsilon_m |\phi_m^{\mathrm{KS}}\rangle \quad \text{with } m \in \mathbb{N}\ ,\ \epsilon_m \leq \epsilon_{m+1}, \tag{25}$$

so that

$$\langle \Psi | \hat{n}_m | \Psi \rangle = 2 \qquad \text{for } m < N \tag{26}$$

$$\langle \Psi | \hat{n}_m | \Psi \rangle = 0 \qquad \text{for } m > N \tag{27}$$

where $\hat{n}_m$ is the number operator for the m-th one-particle eigenstate ϕ_m^{KS}. In second quantization the ground state can be written as

$$|\Psi\rangle = \sum_{i=1}^{N} c_i^\dagger |\Omega\rangle \tag{28}$$

where $c_i^\dagger$ is the creation operator, which creates a particle in the i-th eigenstate of the one particle Schrödinger equation (25)and $|\Omega\rangle$ is the vacuum state. The density $n(\boldsymbol{r})$ is given by

$$n(\boldsymbol{r}) = \langle\Psi|\psi^\dagger(\boldsymbol{r})\psi(\boldsymbol{r})|\Psi\rangle \tag{29}$$

or explicitly in the notation of first quantization by

$$n(\boldsymbol{r}) = \sum_{i=1}^{N} \langle\phi_i^{\mathrm{KS}}|\boldsymbol{r}\rangle \langle\boldsymbol{r}|\phi_i^{\mathrm{KS}}\rangle . \tag{30}$$

The density obtained from equation (30) by solving the one particle Schrödinger equation (25) is a solution to the variational equation (21) under the constraint of

$$\int \delta n(\boldsymbol{r}) d\boldsymbol{r} = 0, \tag{31}$$

which is a rewritten form of equation (14). However, the effective potential $v_{\mathrm{eff}}^{\mathrm{KS}}(\boldsymbol{r})$ depends on the density, thus the Hamiltonian H^{KS} depends on the states ϕ_m^{KS}. For this reason the Kohn-Sham equations (32) have to be solved self consistently:

$$\begin{array}{c} \Big(-\frac{1}{2}\nabla^2 + \underbrace{v(\boldsymbol{r}) + \int \frac{n(\boldsymbol{r}')}{|\boldsymbol{r}-\boldsymbol{r}'|} d\boldsymbol{r}' + \mu_{\mathrm{xc}}(\boldsymbol{r})}_{v_{\mathrm{eff}}^{\mathrm{KS}}} \Big) \phi_m^{\mathrm{KS}}(\boldsymbol{r}) = \epsilon_m \phi_m^{\mathrm{KS}}(\boldsymbol{r}) \\ \circlearrowright \qquad\qquad\qquad\qquad\qquad\qquad \circlearrowright \\ n(\boldsymbol{r}) = 2\sum_{i=1}^{N} |\phi_i^{\mathrm{KS}}(\boldsymbol{r})|^2 \end{array} \tag{32}$$

In practice, good approximations for $\epsilon_{\mathrm{xc}}^{\mathrm{LDA}}(n)$, the energy density per particle, are necessary in order to calculate $\mu_{\mathrm{xc}}^{\mathrm{LDA}}(n(\boldsymbol{r}))$. In applying the theory of the uniform electron gas, the contribution of the exchange energy density per particle $\epsilon_{\mathrm{x}}^{\mathrm{unif}}(n)$ can be evaluated analytically and is given by [7]

$$\epsilon_{\mathrm{x}}^{\mathrm{unif}}(n) = -\frac{3}{4}\left(\frac{3}{\pi}\right)^{1/3} n^{1/3}. \tag{33}$$

In contrast, for $\epsilon_{\mathrm{c}}^{\mathrm{unif}}(n)$ - the correlation energy density per particle of the uniform electron gas - closed analytic expressions are not known. However the behaviour in the limiting cases of very high and low densities is known and very accurate quantum Monte Carlo calculations have been performed for a set of densities in the interstitial region [8]. The usual approach for LDA calculations is to interpolate between the data points of [8] and parametrize $\epsilon_{\mathrm{c}}^{\mathrm{unif}}(n)$ so that the exactly known high and low density behaviour is reproduced. One analytical representation was suggested by Perdew and Wang [9]. In practice the exchange-correlation energy of a crystal can be calculated in the LDA by numerically integrating $n(\epsilon_{\mathrm{x}}^{\mathrm{unif}}(n) + \epsilon_{\mathrm{c}}^{\mathrm{unif}}(n))$ over the unit cell where $\epsilon_c(n)$ is calculated from the approximate analytical representation.

A more sophisticated way to approximate the correlation energy functional is provided by the generalized gradient approximation GGA, where the exchange-correlation functional is approximated as an integral over a function that explicitly depends on the gradient of the density besides the density itself

$$E_{xc}[n] \approx E_{xc}^{\mathrm{GGA}}[n] = \int f(n, \nabla n) d\boldsymbol{r}. \tag{34}$$

A concrete implementation of the GGA for instance was developed by Perdew, Burke and Ernzerhof (PBE) [10].

2.3 Limitations of density functional theory

Density functional theory is a powerful tool to describe the electronic structure on a wide field of applications. It is especially successfully employed in simulations, facilitating research in science and engineering. However the quality of a DFT simulation strongly depends on a good approximation for the exchange correlation energy functional and there are many situation where the commonly used approximations fail to describe the properties of a system correctly. The errors have been traced down to two main sources, namely on the one hand the delocalization error and on the other hand the static correlation error. [11]

The delocalization error is related to the problem of the "self-interaction" that occurs in the description of a single electron, which leads in the many electron case to an analogous problem. For approximate exchange-correlation functionals, this leads to an artificial spreading of the electron density. The problems arise even at such simple cases as the dissociation of the H_2^+ molecule, which should dissociate into a H^+ and H^0 atom. Most DFT functionals however predict two $H^{\frac{1}{2}}$ atoms even at infinite distances. The problem can be traced back to the fact that the approximate exchange correlation

functionals do not exactly cancel the Hartree potential. Hence electrons experience their own Hartree potential so that a delocalized solution is preferred over the localized one.

The static correlation error refers to the problems that occur when dealing with degenerate ground states. In this case a single determinant cannot describe the ground state. Since DFT is based on a single determinant it may result in serious errors for such systems. An example of such a system is the closed shell H_2 molecule at the dissociation limit.

It is also worthwhile mentioning that vdW bonds can never be described accurately by local functionals regarding only one point in space, as vdW interactions always correlate electrons at two points in space.

Summarized, DFT shows issues when dealing with strongly correlated systems or systems where the delocalization errors of DFT are large. This leads in the case of the delcoalization errors to an underestimation of barriers of chemical reactions, the band gaps of materials, the energies of dissociating molecular ions, and charge transfer excitation energies, or in the case of correlated systems to problems in the description of intermolecular interactions, especially van-der-Waals forces, transition metal systems or the breaking of chemical bonds.

While some of these problems may be circumvented by enhancing existing and developing new methods within the DFT framework, others will probably only be solved on the basis of more sophisticated theories. Until the past few years, DFT was despite its drawbacks the dominant method for *ab-initio* simulations of many electron systems, not least because of its low computational complexity. However, the opportunities provided by modern computer facilities combined with recent methodical advances offer the possibility to extend *ab-initio* simulations to more advanced methods. Hence the prospect is good that many systems which cannot be treated correctly with DFT will become accessible in the near future, by means of feasible computer simulations. One promising approach is the random phase approximation, which offers a promising method to describe correlated systems.

3 The Random Phase Approximation (RPA)

3.1 The Adiabatic Connection Fluctuation-Dissipation Theorem (ACFDT)

In the previous section, it was shown that Kohn-Sham density functional theory is an approach to approximate the Schrödinger equation of a system of interacting electrons in an external potential by mapping the problem onto a system of non-interacting electrons in an effective potential. The crucial step in DFT is to find a good approximation for the exchange-correlation energy E_{xc}. The following section deals with the derivation of an alternative expression for E_{xc}. The general idea of the adiabatic connection fluctuation-dissipation theorem is to derive E_{xc} by observing a series of systems which emanate from turning the fully interacting Hamiltonian smoothly into the Kohn Sham Hamiltonian. This process is described by introducing a parameter λ, which governs the electron-electron interaction as well as the effective potential in the Hamiltonian $H(\lambda)$. The adiabatic connection fluctuation-dissipation theorem states that the exchange - correlation energy can be written as [12][13][14]

$$E_{\mathrm{xc}} = -\frac{1}{2}\int_0^1 d\lambda \int d^3\boldsymbol{r} d^3\boldsymbol{r}' \frac{1}{|\boldsymbol{r}-\boldsymbol{r}'|}\left(n(\boldsymbol{r})\delta(\boldsymbol{r}-\boldsymbol{r}') + \frac{1}{\pi}\int_0^\infty d\omega \chi^\lambda(\boldsymbol{r},\boldsymbol{r}',\mathrm{i}\,\omega)\right), \quad (35)$$

where the index λ indicates that the quantities are related to the system with Hamiltonian $H(\lambda)$ and where $\chi^\lambda(\boldsymbol{r},\boldsymbol{r}',\omega)$ is the linear response function, describing changes in the density due to fluctuations of the external potential in first order. The linear response function will be discussed in more detail later in this section, when the fluctuation-dissipation theorem is derived.

In the following the theorem stated in equation (35) shall be proofed. First it will be shown that an integral with respect to λ of the expectation value of the electron-electron interaction in the λ dependent ground state will yield the exchange correlation energy. This is referred to as the adiabatic connection. In a second step, this integral is expressed in terms of the analytic continuation of the linear response function $\chi^\lambda(\boldsymbol{r},\boldsymbol{r}',\mathrm{i}\,\omega)$ representing the fluctuation-dissipation part of the adiabatic connection fluctuation-dissipation theorem.

The Hamiltonian $H(\lambda)$ shall be of a form that adiabatically connects the Kohn-Sham system of non interacting electrons with the real many electron system of full electron-electron interaction. It is therefore defined in the following way:

$$H(\lambda) = T + V(\lambda) + \lambda V_{\mathrm{ee}}, \quad (36)$$

where the real space representation of the operators V_{ee} and V_λ are given by

$$V_{\text{ee}} = \sum_{i<j} \frac{1}{|\boldsymbol{r}_i - \boldsymbol{r}_j|} \tag{37}$$

and

$$V(\lambda) = \sum_i v_\lambda(\boldsymbol{r}_i) \tag{38}$$

i, j numbering the electrons.

In equation (36) the electron-electron coupling V_{ee} is scaled by the coupling constant λ. Hence, a value of $\lambda = 1$ yields the correct fully interacting Hamiltonian, if the effective potential v_1 equals the external potential v

$$v_1(\boldsymbol{r}) = v(\boldsymbol{r}). \tag{39}$$

We require that the electron densities obtained from all different ground states $|\Psi(\lambda)\rangle$ of all Hamiltonians $H(\lambda)$ are all equal to each other,

$$\langle\Psi(\lambda)|\psi^\dagger(\boldsymbol{r})\psi(\boldsymbol{r})|\Psi(\lambda)\rangle \stackrel{!}{=} \langle\Psi(1)|\psi^\dagger(\boldsymbol{r})\psi(\boldsymbol{r})|\Psi(1)\rangle = n(\boldsymbol{r}) \quad \forall\lambda. \tag{40}$$

Therefore, the potential $v_\lambda(\boldsymbol{r})$ has to be chosen such that the ground state density $n(\boldsymbol{r})$ is independent of λ and its value equals the value of the fully interacting system. It follows from equation (40) that the effective potential for $\lambda = 0$ is the already discussed Kohn-Sham effective potential

$$v_0(\boldsymbol{r}) = v_{\text{eff}}^{\text{KS}}(\boldsymbol{r}). \tag{41}$$

For the Kohn-Sham system equation (17) can be rearranged to

$$E_{\text{H}} + E_{\text{xc}} = E - E_{\text{ext}} - T_s. \tag{42}$$

Now the energy for both systems, the fully interacting system $\lambda = 1$ and the Kohn-Sham system $\lambda = 0$, must be equal due to the Hohenberg-Kohn theorems. Therefore $E - E_{\text{ext}}$ can be written in terms of the fully interacting system as

$$E - E_{\text{ext}} = \langle\Psi(1)|H(1)|\Psi(1)\rangle - \langle\Psi(1)|V(1)|\Psi(1)\rangle\,, \tag{43}$$

while T_s can be written as

$$T_s = \langle\Psi(0)|T|\Psi(0)\rangle = \langle\Psi(0)|H(0) - V(0)|\Psi(0)\rangle\,. \tag{44}$$

Inserting (43) and (44) into (42) yields

$$E_{\mathrm{Hxc}} \equiv E_{\mathrm{H}} + E_{\mathrm{xc}} = \langle\Psi(1)|H(1) - V(1)|\Psi(1)\rangle - \langle\Psi(0)|H(0) - V(0)|\Psi(0)\rangle \tag{45}$$

$$= \int_0^1 d\lambda \frac{d}{d\lambda} \langle\Psi(\lambda)|H(\lambda) - V(\lambda)|\Psi(\lambda)\rangle \,. \tag{46}$$

To simplify this expression (46) one can exploit the Hellmann-Feynman theorem which states

$$\frac{d}{d\lambda}E(\lambda) = \langle\psi(\lambda)|\frac{dH(\lambda)}{d\lambda}|\psi(\lambda)\rangle \tag{47}$$

where $H(\lambda)$ is a Hamiltonian parametrized by λ and $|\psi(\lambda)\rangle$ is its normalized eigenstate with the eigenvalue E. The theorem may be proofed formally in the following way:

$$\frac{dE(\lambda)}{d\lambda} = \frac{d}{d\lambda} \langle\phi(\lambda)|H(\lambda)|\phi(\lambda)\rangle \tag{48}$$

$$= \langle\frac{d\phi(\lambda)}{d\lambda}|H(\lambda)|\phi(\lambda)\rangle + \langle\phi(\lambda)|\frac{dH(\lambda)}{d\lambda}|\phi(\lambda)\rangle + \langle\phi(\lambda)|H(\lambda)|\frac{d\phi(\lambda)}{d\lambda}\rangle \tag{49}$$

$$= E\left(\langle\frac{d\phi(\lambda)}{d\lambda}|\phi(\lambda)\rangle + \langle\phi(\lambda)|\frac{d\phi(\lambda)}{d\lambda}\rangle\right) + \langle\phi(\lambda)|\frac{dH(\lambda)}{d\lambda}|\phi(\lambda)\rangle \tag{50}$$

$$= E\underbrace{\frac{d}{d\lambda}\langle\phi(\lambda)|\phi(\lambda)\rangle}_{=0} + \langle\phi(\lambda)|\frac{dH(\lambda)}{d\lambda}|\phi(\lambda)\rangle \tag{51}$$

$$= \langle\phi(\lambda)|\frac{dH(\lambda)}{d\lambda}|\phi(\lambda)\rangle \tag{52}$$

From equation (48) to (49) the product rule was simply applied. Equation (50) follows from (49) by the fact that $\phi(\lambda)$ are eigenstates of $H(\lambda)$. Since $\langle\phi(\lambda)|\phi(\lambda)\rangle = 1$ for all λ, the first term in equation (51) vanishes.

Another useful statement regarding the expectation value of a local potential operator with respect to different states with the same density $\langle\Psi(\lambda)|V_{\mathrm{local}}(\lambda)|\Psi(\lambda)\rangle$ is shown in equation (53) to (57),

$$V_{\mathrm{local}}(\lambda) = v_{\mathrm{local}}(\lambda, \boldsymbol{r})\psi^\dagger(\boldsymbol{r})\psi(\boldsymbol{r}). \tag{53}$$

Here $v(\boldsymbol{r})$ is just a scalar function and $\psi^\dagger(\boldsymbol{r})$ and $\psi(\boldsymbol{r})$ are the usual field operators. The different states $\Psi(\lambda)$ are parametrized by λ and do all have the same density, as

stated in equation (40). Then

$$\frac{d}{d\lambda}\langle\Psi(\lambda)|V_{\text{local}}(\lambda)|\Psi(\lambda)\rangle = \frac{d}{d\lambda}\int v_{\text{local}}(\lambda,\boldsymbol{r})\,\langle\Psi(\lambda)|\psi^{\dagger}(\boldsymbol{r})\psi(\boldsymbol{r})|\Psi(\lambda)\rangle\,d^3\boldsymbol{r} \tag{54}$$

$$= \frac{d}{d\lambda}\int v_{\text{local}}(\lambda,\boldsymbol{r})n(\boldsymbol{r})d^3\boldsymbol{r} \tag{55}$$

$$= \int \frac{dv_{\text{local}}(\lambda,\boldsymbol{r})}{d\lambda}n(\boldsymbol{r})d^3\boldsymbol{r} \tag{56}$$

$$= \langle\Psi(\lambda)|\frac{dV_{\text{local}}(\lambda)}{d\lambda}|\Psi(\lambda)\rangle\,. \tag{57}$$

Going back to equation (46) one may now easily evaluate the integrand by using the Hellmann-Feynman theorem (47).

$$\frac{d}{d\lambda}\langle\Psi(\lambda)|H(\lambda)-V(\lambda)|\Psi(\lambda)\rangle = \frac{d}{d\lambda}\langle\Psi(\lambda)|H(\lambda)|\Psi(\lambda)\rangle - \frac{d}{d\lambda}\langle\Psi(\lambda)|V(\lambda)|\Psi(\lambda)\rangle \tag{58}$$

$$= \langle\Psi(\lambda)|\frac{dH(\lambda)}{d\lambda}|\Psi(\lambda)\rangle - \langle\Psi(\lambda)|\frac{d}{d\lambda}V(\lambda)|\Psi(\lambda)\rangle \tag{59}$$

$$= \langle\Psi(\lambda)|\frac{d(T+\lambda V_{\text{ee}})}{d\lambda}|\Psi(\lambda)\rangle \tag{60}$$

$$= \langle\Psi(\lambda)|V_{\text{ee}}|\Psi(\lambda)\rangle \tag{61}$$

$$\Rightarrow E_{\text{Hxc}} = \int_0^1 d\lambda\,\langle\Psi(\lambda)|V_{\text{ee}}|\Psi(\lambda)\rangle \tag{62}$$

From equation (58) to (59), the Hellmann-Feynman theorem was applied to the left term and the right term was evaluated by using the fact that the density is independent of λ and $V(\lambda)$ is only a local potential operator, see equation (53)to (57). To obtain equation (60) from (59), H was substituted in accordance with equation (36).

Before expression (62) is reformulated by applying the fluctuation-dissipation theorem [15], the linear response function χ shall be introduced briefly. The linear response function, also called polarizability, describes the reaction of a system to a small perturbation to the external potential δv_{ext}. In the case of the Kohn-Sham system, which is a system of non-interacting particles, the response function is called independent particle polarizability χ^0 (or often χ^{KS}) and describes the response due to a small change in the effective potential $\delta v_{\text{eff}}^{\text{KS}}$. The density difference between the perturbed and unperturbed system at a given time t is denoted by $\delta n(\boldsymbol{r},t) \equiv n_{\text{per}}(\boldsymbol{r},t) - n_0(\boldsymbol{r})$. Its Fourier transform $\delta n(\boldsymbol{r},\omega)$ is indicated by the replacement of the time variable t by ω. Hence the

density of the perturbed system $n_{\text{per}}(\boldsymbol{r},t)$ is related to the unperturbed density $n_0(\boldsymbol{r})$ in the following way

$$n_{\text{per}}(\boldsymbol{r},t) = n_0(\boldsymbol{r}) + \delta n(\boldsymbol{r},t) \tag{63}$$

$$= n_0(\boldsymbol{r}) + \int d\omega\, e^{-\mathrm{i}\,\omega t}\delta n(\boldsymbol{r},\omega) \tag{64}$$

Within linear response theory, $\delta n(\boldsymbol{r},t)$ can be calculated from the small external perturbations $\delta v(\boldsymbol{r},t')$ and the linear response function $\chi(\boldsymbol{r},\boldsymbol{r}',t-t')$ as

$$\delta n(\boldsymbol{r},t) = \int dt' \int d^3\boldsymbol{r}\; \chi(\boldsymbol{r},\boldsymbol{r}',t-t')\delta v(\boldsymbol{r},t'). \tag{65}$$

In other words, $\chi(\boldsymbol{r},\boldsymbol{r}',t-t')$ is the functional derivative of $n(\boldsymbol{r},t)$ with respect to $v(\boldsymbol{r}',t')$:

$$\chi(\boldsymbol{r},\boldsymbol{r}',t-t') = \frac{\delta n(\boldsymbol{r},t)}{\delta v(\boldsymbol{r}',t')}. \tag{66}$$

In references [7], [16] and [17] an explicit expression for the response function $\chi(\boldsymbol{r},\boldsymbol{r}',t-t')$ can be found and is given by

$$\chi(\boldsymbol{r},\boldsymbol{r}',t-t') = -i\theta(t-t')\left\langle\Psi_0|[n(\boldsymbol{r},t),n(\boldsymbol{r}',t')]|\Psi_0\right\rangle, \tag{67}$$

where Ψ_0 is the ground state of the unperturbed system, $[,]$ is the commutator and $n(\boldsymbol{r},t)$ is the density operator in the Heisenberg picture

$$n(\boldsymbol{r},t) = e^{\mathrm{i}\,Ht}n(\boldsymbol{r})e^{-\mathrm{i}\,Ht} \tag{68}$$

Similar expressions can be found for the frequency domain of the response function $\chi(\boldsymbol{r},\boldsymbol{r}',\omega)$ and the other Fourier transforms of the quantities of interest:

$$\delta n(\boldsymbol{r},\omega) = \int d\boldsymbol{r}'\chi(\boldsymbol{r},\boldsymbol{r}',\omega)\delta v(\boldsymbol{r}',\omega) \tag{69}$$

$$\chi(\boldsymbol{r},\boldsymbol{r}',\omega) = \frac{\delta n(\boldsymbol{r},\omega)}{\delta v(\boldsymbol{r}',\omega)} \tag{70}$$

$$= \mathcal{F}[\chi(\boldsymbol{r},\boldsymbol{r}',t)](\omega). \tag{71}$$

In order to evaluate equation (71), a slight modification of equation (67) is necessary. To get a well defined function from the Fourier transform of $\chi(\boldsymbol{r},\boldsymbol{r}',t-t')$ a factor

$e^{-\eta(t-t')}$ has to be introduced, where η is a positive infinitesimal. For all calculations the limit $\eta \to 0^+$ is performed as the final step, after all other limits are evaluated. From a physical point of view, the property $\lim\limits_{(t-t')\to\infty} e^{-\eta(t-t')} = 0$ has no relevance for the description of the system, as in any experimental realisation one deals with finite time periods and hence the factor $e^{-\eta(t-t')} = 1$ for all times considered. This can be seen in detail from equation (65), assuming that the system was originally unperturbed or in other words $\delta v(\boldsymbol{r}', t') = 0 \quad \forall\, t' < T$ where T is the time when the perturbation started. In that case, the factor $e^{-\eta(t-t')}$ does not affect the density variation $\delta n(\boldsymbol{r}, t)$

$$\chi(\boldsymbol{r}, \boldsymbol{r}', \omega) \stackrel{!}{=} \lim_{\eta\to 0^+} \mathcal{F}[\chi(\boldsymbol{r}, \boldsymbol{r}', t) e^{-\eta t}](\omega). \tag{72}$$

In what follows, the limit $\eta \to 0^+$ is assumed implicitly and not written out any more:

$$\chi(\boldsymbol{r}, \boldsymbol{r}', \omega) = \int_{-\infty}^{\infty} e^{\mathrm{i}\, t\omega} \chi(\boldsymbol{r}, \boldsymbol{r}', t) e^{-\eta t} dt \tag{73}$$

$$= -\,\mathrm{i} \int_{-\infty}^{\infty} e^{\mathrm{i}\, t(\omega + \mathrm{i}\,\eta)} \theta(t)\, \langle \Psi_0 | [n(\boldsymbol{r}, t), n(\boldsymbol{r}', 0)] | \Psi_0 \rangle\, dt \tag{74}$$

$$= -\,\mathrm{i} \int_{0}^{\infty} e^{\mathrm{i}\, t(\omega + \mathrm{i}\,\eta)} \big(\langle \Psi_0 | e^{\mathrm{i}\, Ht} n(\boldsymbol{r}) e^{-\,\mathrm{i}\, Ht} n(\boldsymbol{r}') | \Psi_0 \rangle -$$

$$- \langle \Psi_0 | n(\boldsymbol{r}') e^{\mathrm{i}\, Ht} n(\boldsymbol{r}) e^{-\,\mathrm{i}\, Ht} | \Psi_0 \rangle \big) dt. \tag{75}$$

So far equation (67) was inserted in equation (72) and the commutator was written out explicitly while the θ-function was passed to the integration limits. Since the eigenfunctions of the Hamiltonian form a complete orthonormal basis set, equation (77) is obtained from equation (75) by inserting the eigendecomposition of the Hamiltonian exponentials and using $\langle \Psi_0 | \Psi_j \rangle = \delta_{0j}$:

$$\chi(\boldsymbol{r}, \boldsymbol{r}', \omega) = -\,\mathrm{i} \int_{0}^{\infty} e^{\mathrm{i}\, t(\omega + \mathrm{i}\,\eta)} \big(\langle \Psi_0 | e^{\mathrm{i}\, E_0 t} n(\boldsymbol{r}) \sum_j e^{-\,\mathrm{i}\, E_j t} \, |\Psi_j\rangle \, \langle \Psi_j | \, n(\boldsymbol{r}') | \Psi_0 \rangle -$$

$$- \langle \Psi_0 | n(\boldsymbol{r}') \sum_j e^{\mathrm{i}\, E_j t} \, |\Psi_j\rangle \, \langle \Psi_j | \, n(\boldsymbol{r}) e^{-\,\mathrm{i}\, E_0 t} | \Psi_0 \rangle \big) dt \tag{76}$$

$$= -\,\mathrm{i} \sum_j \langle \Psi_0 | n(\boldsymbol{r}) | \Psi_j \rangle \, \langle \Psi_j | n(\boldsymbol{r}') | \Psi_0 \rangle \int_0^{\infty} e^{\mathrm{i}\, t(\omega + \mathrm{i}\,\eta - (E_j - E_0))} dt -$$

$$- \langle \Psi_0 | n(\boldsymbol{r}') | \Psi_j \rangle \, \langle \Psi_j | n(\boldsymbol{r}) | \Psi_0 \rangle \int_0^{\infty} e^{\mathrm{i}\, t(\omega + \mathrm{i}\,\eta + (E_j - E_0))} dt. \tag{77}$$

For $j = 0$ the two terms cancel each other out so that after the replacement $(E_j - E_0) = \omega_j$ one obtains

$$\chi(\boldsymbol{r}, \boldsymbol{r}', \omega) = -\sum_{j\neq 0} \langle\Psi_0|n(\boldsymbol{r})|\Psi_j\rangle \langle\Psi_j|n(\boldsymbol{r}')|\Psi_0\rangle \left.\frac{e^{\mathrm{i}\, t(\omega-\omega_j)} e^{-\eta t}}{\omega + \mathrm{i}\,\eta - \omega_j}\right|_{t=0}^{\infty} -$$

$$- \langle\Psi_0|n(\boldsymbol{r}')|\Psi_j\rangle \langle\Psi_j|n(\boldsymbol{r})|\Psi_0\rangle \left.\frac{e^{\mathrm{i}\, t(\omega+\omega_j)} e^{-\eta t}}{\omega + \mathrm{i}\,\eta + \omega_j}\right|_{t=0}^{\infty} \tag{78}$$

$$= \sum_{j\neq 0} \frac{\langle\Psi_0|n(\boldsymbol{r})|\Psi_j\rangle \langle\Psi_j|n(\boldsymbol{r}')|\Psi_0\rangle}{\omega + \mathrm{i}\,\eta - \omega_j} - \frac{\langle\Psi_0|n(\boldsymbol{r}')|\Psi_j\rangle \langle\Psi_j|n(\boldsymbol{r})|\Psi_0\rangle}{\omega + \mathrm{i}\,\eta + \omega_j}. \tag{79}$$

In the case of a non-interacting system of N fermions, equation (79) can be written in terms of the single particle energy eigenfunctions $\phi_n(\boldsymbol{r})$ and the corresponding eigenvalues ϵ_n, where $\epsilon_n \leq \epsilon_{n+1}$. In the ground state, the lowest N energy eigenstates are occupied with one particle, all other states are unoccupied. In second quantization, the density operator of a system of non-interacting particles may be written as

$$n(\boldsymbol{r}) = \sum_{n,m} \phi_n^*(\boldsymbol{r})\phi_m(\boldsymbol{r}) \mathrm{a}_n^\dagger \mathrm{a}_m \tag{80}$$

where $\mathrm{a}_n^\dagger$ and a_n are energy eigenstate creation and annihilation operators. In the next step, $\langle\Psi_j|n(\boldsymbol{r})|\Psi_0\rangle$ is evaluated.

$$\langle\Psi_j|n(\boldsymbol{r})|\Psi_0\rangle = \sum_{n,m} \phi_n^*(\boldsymbol{r})\phi_m(\boldsymbol{r}) \langle\Psi_j|\mathrm{a}_n^\dagger \mathrm{a}_m|\Psi_0\rangle \tag{81}$$

The addends in the above expression yield 0 if $m > N$, since the ground state does not posses particles above the one electron state ϕ_N that may be annihilated. Now we exploit the anti-commutator relations for $\mathrm{a}_n^\dagger$ and a_m which are given by

$$\left\{\mathrm{a}_n, \mathrm{a}_m\right\} = \left\{\mathrm{a}_m^\dagger, \mathrm{a}_n^\dagger\right\} = 0 \quad ; \quad \left\{\mathrm{a}_n^\dagger, \mathrm{a}_m\right\} = \delta_{m,n} \tag{82}$$

so that

$$\langle\Psi_j|n(\boldsymbol{r})|\Psi_0\rangle = \sum_{\substack{n \\ m\leq N}} \phi_n^*(\boldsymbol{r})\phi_m(\boldsymbol{r}) \left(\langle\Psi_j|\delta_{n,m}|\Psi_0\rangle - \langle\Psi_j|\mathrm{a}_m \mathrm{a}_n^\dagger|\Psi_0\rangle\right). \tag{83}$$

For $j \neq 0$, the term with $\delta_{n,m}$ vanishes since the Ψ_j are orthogonal to each other. The term $\langle\Psi_j|\mathrm{a}_m \mathrm{a}_n^\dagger|\Psi_0\rangle$ vanishes for all $n \leq N$, because the states below ϕ_{N+1} are already occupied in the ground state so that the creation operator $\mathrm{a}_n^\dagger$ applied to the ground

state yields 0 for $n \leq N$. Hence,

$$\langle \Psi_j | n(\boldsymbol{r}) | \Psi_0 \rangle = - \sum_{\substack{n>N \\ m \leq N}} \phi_n^*(\boldsymbol{r}) \phi_m(\boldsymbol{r}) \langle \Psi_j | \mathrm{a}_m \mathrm{a}_n^\dagger | \Psi_0 \rangle \quad \forall j \neq 0. \tag{84}$$

In the following, $m \leq N$ will be denoted as "$m \in$ occ", indicating energy levels occupied in the ground state, while $n > N$ will be denoted as "$n \in$ uocc" indicating energy levels unoccupied in the ground state.

Let M_{sx} be the set of "single" excited states, which differ from the ground state only by single particle lifted from energy ϵ_m to ϵ_n.

$$M_{\mathrm{sx}} = \left\{ |\Psi_{nm}\rangle = \mathrm{a}_m \mathrm{a}_n^\dagger |\Psi_0\rangle : m \in \mathrm{occ}, n \in \mathrm{uocc} \right\} \tag{85}$$

Now $\mathrm{a}_m \mathrm{a}_n^\dagger |\Psi_0\rangle$ in equation (84) is an excited state $|\Psi_j\rangle \in M_{\mathrm{sx}}$. Since the $|\Psi_j\rangle$ form an orthonormal basis,

$$\langle \Psi_j | \mathrm{a}_m \mathrm{a}_n^\dagger | \Psi_0 \rangle = \begin{cases} \delta_{k,n}\delta_{l,m} & : \langle \Psi_j | = \langle \Psi_0 | \, \mathrm{a}_k \mathrm{a}_l^\dagger = \langle \Psi_{kl} | \in M_{\mathrm{sx}}^\dagger \quad \text{(i)} \\ \delta_{n,m} & : \langle \Psi_j | = \langle \Psi_0 | \text{ and } n, m \in \mathrm{uocc} \quad \text{(ii)} \\ 0 & : \text{else} \quad \text{(iii)} \end{cases} \tag{86}$$

This means that for $\chi^0(\boldsymbol{r}, \boldsymbol{r}', \omega)$, the density-density response function of a system of non-interacting fermions, the sum over all excited states in equation (79) is reduced to the sum over all "single" excited states $|\Psi_{nm}\rangle \in M_{\mathrm{sx}}$. The energy difference between the ground state and an excited state $|\Psi_{nm}\rangle$ is just given by $\omega_j = E_j - E_0 = \epsilon_n - \epsilon_m$ so that in equation (79) the replacement

$$\sum_{j \neq 0} \frac{|\Psi_j\rangle \langle \Psi_j|}{\omega + \mathrm{i}\,\eta \pm \omega_j} \to \sum_{\substack{n \in \mathrm{uocc} \\ m \in \mathrm{occ}}} \frac{|\Psi_{nm}\rangle \langle \Psi_{nm}|}{\omega + \mathrm{i}\,\eta \pm (\epsilon_n - \epsilon_m)} \tag{87}$$

can be done. Evaluating equation (84) for $\Psi_j = \Psi_{nm}$ one gets

$$\langle \Psi_{nm} | n(\boldsymbol{r}) | \Psi_0 \rangle = - \sum_{k,l} \phi_k^*(\boldsymbol{r}) \phi_l(\boldsymbol{r}) \langle \Psi_{nm} | \mathrm{a}_l \mathrm{a}_k^\dagger | \Psi_0 \rangle = -\phi_n^*(\boldsymbol{r}) \phi_m(\boldsymbol{r}) \tag{88}$$

so that finally

$$\chi^0(\boldsymbol{r}, \boldsymbol{r}', \omega) = \sum_{\substack{n \in \mathrm{uocc} \\ m \in \mathrm{occ}}} \frac{\phi_n(\boldsymbol{r}) \phi_m^*(\boldsymbol{r}) \phi_n^*(\boldsymbol{r}') \phi_m(\boldsymbol{r}')}{\omega + \mathrm{i}\,\eta - \epsilon_n + \epsilon_m} - \frac{\phi_n(\boldsymbol{r}') \phi_m^*(\boldsymbol{r}') \phi_n^*(\boldsymbol{r}) \phi_m(\boldsymbol{r})}{\omega + \mathrm{i}\,\eta + \epsilon_n - \epsilon_m} \tag{89}$$

Now after the density-density response function χ was introduced and explicit forms

were presented in equation (67), (79) and (89), the result from the adiabatic connection, equation (62), will be reformulated in terms of χ.

First the expectation value of the electron-electron Coulomb interaction is written in terms of a spatial integration of the expectation value of density operators. The following anti-commutator relations hold for fermionic field operators [7][16], compare also equation (82):

$$\{\psi(\boldsymbol{r}), \psi(\boldsymbol{r}')\} = \left\{\psi^\dagger(\boldsymbol{r}), \psi^\dagger(\boldsymbol{r}')\right\} = 0 \quad ; \quad \left\{\psi^\dagger(\boldsymbol{r}), \psi(\boldsymbol{r}')\right\} = \delta^{(3)}(\boldsymbol{r} - \boldsymbol{r}'). \tag{90}$$

The electron-electron interaction operator is given by

$$V_{\text{ee}} = \frac{1}{2} \int \frac{1}{|\boldsymbol{r} - \boldsymbol{r}'|} \psi^\dagger(\boldsymbol{r}) \psi^\dagger(\boldsymbol{r}') \psi(\boldsymbol{r}') \psi(\boldsymbol{r}) d^3\boldsymbol{r} d^3\boldsymbol{r}'. \tag{91}$$

The field operators can be rearranged by using the relation in equation (90)

$$\psi^\dagger(\boldsymbol{r}) \psi^\dagger(\boldsymbol{r}') \psi(\boldsymbol{r}') \psi(\boldsymbol{r}) = -\psi^\dagger(\boldsymbol{r}) \psi^\dagger(\boldsymbol{r}') \psi(\boldsymbol{r}) \psi(\boldsymbol{r}') \tag{92}$$

$$= -\psi^\dagger(\boldsymbol{r}) \left(\delta^{(3)}(\boldsymbol{r} - \boldsymbol{r}') - \psi(\boldsymbol{r}) \psi^\dagger(\boldsymbol{r}')\right) \psi(\boldsymbol{r}') \tag{93}$$

$$= \psi^\dagger(\boldsymbol{r}) \psi(\boldsymbol{r}) \psi^\dagger(\boldsymbol{r}') \psi(\boldsymbol{r}') - \delta^{(3)}(\boldsymbol{r} - \boldsymbol{r}') \psi^\dagger(\boldsymbol{r}) \psi(\boldsymbol{r}') \tag{94}$$

$$= \hat{n}(\boldsymbol{r}) \hat{n}(\boldsymbol{r}') - \delta^{(3)}(\boldsymbol{r} - \boldsymbol{r}') \hat{n}(\boldsymbol{r}, \boldsymbol{r}'). \tag{95}$$

Note that in equation (95), $\hat{n}(\boldsymbol{r})$ denotes the density operator $\hat{n}(\boldsymbol{r}, \boldsymbol{r}') = \psi^\dagger(\boldsymbol{r}) \psi(\boldsymbol{r}')$, not the groundstate density. For the remainder of this section the hat symbol " ˆ " will be used to address the density operator directly, since it might be easily confused with the groundstate density $n(\boldsymbol{r})$ at this point. However the hat symbol for operators will be omitted again later as it should then be clear from the context, whether the density operator or the groundstate density is meant with $n(\boldsymbol{r})$. With the previous result,

equation (62) can be rewritten to

$$E_{\text{Hxc}} = \int_0^1 d\lambda \, \langle \Psi(\lambda) | V_{\text{ee}} | \Psi(\lambda) \rangle \tag{96}$$

$$= \int_0^1 d\lambda \, \langle \Psi(\lambda) | \frac{1}{2} \int d^3\boldsymbol{r} d^3\boldsymbol{r}' \frac{1}{|\boldsymbol{r} - \boldsymbol{r}'|} \left(\hat{n}(\boldsymbol{r}) \hat{n}(\boldsymbol{r}') - \delta^{(3)}(\boldsymbol{r} - \boldsymbol{r}') \hat{n}(\boldsymbol{r}, \boldsymbol{r}') \right) | \Psi(\lambda) \rangle \tag{97}$$

$$= \frac{1}{2} \int_0^1 d\lambda \int d^3\boldsymbol{r} d^3\boldsymbol{r}' \frac{1}{|\boldsymbol{r} - \boldsymbol{r}'|} \langle \Psi(\lambda) | \frac{\hat{n}(\boldsymbol{r}) \hat{n}(\boldsymbol{r}')}{2} - \delta^{(3)}(\boldsymbol{r} - \boldsymbol{r}') \hat{n}(\boldsymbol{r}, \boldsymbol{r}') | \Psi(\lambda) \rangle +$$

$$+ \frac{1}{2} \int_0^1 d\lambda \int d^3\boldsymbol{r}' d^3\boldsymbol{r} \frac{1}{|\boldsymbol{r}' - \boldsymbol{r}|} \langle \Psi(\lambda) | \frac{\hat{n}(\boldsymbol{r}') \hat{n}(\boldsymbol{r})}{2} | \Psi(\lambda) \rangle \tag{98}$$

$$= \frac{1}{2} \int_0^1 d\lambda \int d^3\boldsymbol{r} d^3\boldsymbol{r}' \frac{1}{|\boldsymbol{r} - \boldsymbol{r}'|} \langle \Psi(\lambda) | \frac{\hat{n}(\boldsymbol{r}) \hat{n}(\boldsymbol{r}') + \hat{n}(\boldsymbol{r}') \hat{n}(\boldsymbol{r})}{2} - \delta^{(3)}(\boldsymbol{r} - \boldsymbol{r}') \hat{n}(\boldsymbol{r}, \boldsymbol{r}') | \Psi(\lambda) \rangle \tag{99}$$

To get from equation (97) to equation (99), 1/2 was factored out of the product $\hat{n}(\boldsymbol{r})\hat{n}(\boldsymbol{r}')$ and the integration variables $\boldsymbol{r}$ and $\boldsymbol{r}'$ were interchanged in the second term. The order of integration in the second term is then reversed so that it coincides with the order of the first term. Finally $\boldsymbol{r}$ and $\boldsymbol{r}'$ in $\frac{1}{|\boldsymbol{r}' - \boldsymbol{r}|}$ can be interchanged since it is symmetric and the two terms can be merged together again. Now in order to express $\langle \Psi(\lambda) | \hat{n}(\boldsymbol{r}) \hat{n}(\boldsymbol{r}') + \hat{n}(\boldsymbol{r}') \hat{n}(\boldsymbol{r}) | \Psi(\lambda) \rangle$ in terms of the polarizability χ it is useful to

examine the following expression:

$$\chi(\boldsymbol{r},\boldsymbol{r}',\mathrm{i}\,\omega)+\chi(\boldsymbol{r}',\boldsymbol{r},\mathrm{i}\,\omega)=$$

$$=\sum_{j\neq 0}\frac{\langle\Psi_0|\hat{n}(\boldsymbol{r})|\Psi_j\rangle\langle\Psi_j|\hat{n}(\boldsymbol{r}')|\Psi_0\rangle}{\mathrm{i}\,\omega+\mathrm{i}\,\eta-\omega_j}-\frac{\langle\Psi_0|\hat{n}(\boldsymbol{r}')|\Psi_j\rangle\langle\Psi_j|\hat{n}(\boldsymbol{r})|\Psi_0\rangle}{\mathrm{i}\,\omega+\mathrm{i}\,\eta+\omega_j}+$$

$$+\frac{\langle\Psi_0|\hat{n}(\boldsymbol{r}')|\Psi_j\rangle\langle\Psi_j|\hat{n}(\boldsymbol{r})|\Psi_0\rangle}{\mathrm{i}\,\omega+\mathrm{i}\,\eta-\omega_j}-\frac{\langle\Psi_0|\hat{n}(\boldsymbol{r})|\Psi_j\rangle\langle\Psi_j|\hat{n}(\boldsymbol{r}')|\Psi_0\rangle}{\mathrm{i}\,\omega+\mathrm{i}\,\eta+\omega_j} \tag{100}$$

$$=\sum_{j\neq 0}\Big(\langle\Psi_0|\hat{n}(\boldsymbol{r})|\Psi_j\rangle\langle\Psi_j|\hat{n}(\boldsymbol{r}')|\Psi_0\rangle+\langle\Psi_0|\hat{n}(\boldsymbol{r}')|\Psi_j\rangle\langle\Psi_j|\hat{n}(\boldsymbol{r})|\Psi_0\rangle\Big)\times$$

$$\times\left(\frac{1}{\mathrm{i}\,\omega+\mathrm{i}\,\eta-\omega_j}-\frac{1}{\mathrm{i}\,\omega+\mathrm{i}\,\eta+\omega_j}\right) \tag{101}$$

$$=-\sum_{j\neq 0}\Big(\langle\Psi_0|\hat{n}(\boldsymbol{r})|\Psi_j\rangle\langle\Psi_j|\hat{n}(\boldsymbol{r}')|\Psi_0\rangle+\langle\Psi_0|\hat{n}(\boldsymbol{r}')|\Psi_j\rangle\langle\Psi_j|\hat{n}(\boldsymbol{r})|\Psi_0\rangle\Big)\times$$

$$\times\frac{2\omega_j}{(\omega+\eta)^2+\omega_j^2} \tag{102}$$

The factor containing ω is subject to the following calculation:

$$\int_0^\infty\frac{2\omega_j}{(\omega+\eta)^2+\omega_j^2}d\omega=\frac{2}{\omega_j}\int_0^\infty\frac{1}{1+\left(\frac{(\omega+\eta)}{\omega_j}\right)^2}d\omega \tag{103}$$

$$=2\int_{\frac{\eta}{\omega_j}}^\infty\frac{1}{1+w'^2}d\omega' \tag{104}$$

$$=2\arctan(\omega')\Big|_{\frac{\eta}{\omega_j}}^\infty \tag{105}$$

$$=\pi \tag{106}$$

where from equation (105) to (106) the limit $\eta\to 0^+$ was performed. With this result we get

$$\int_0^\infty\chi(\boldsymbol{r}',\boldsymbol{r},\mathrm{i}\,\omega)+\chi(\boldsymbol{r},\boldsymbol{r}',\mathrm{i}\,\omega)\;d\omega=$$

$$-\pi\sum_{j\neq 0}\langle\Psi_0|\hat{n}(\boldsymbol{r})|\Psi_j\rangle\langle\Psi_j|\hat{n}(\boldsymbol{r}')|\Psi_0\rangle+\langle\Psi_0|\hat{n}(\boldsymbol{r}')|\Psi_j\rangle\langle\Psi_j|\hat{n}(\boldsymbol{r})|\Psi_0\rangle\,. \tag{107}$$

Note that this is valid for all ground states Ψ_0 and excited states Ψ_j of any Hamiltonian, therefore also for the Hamiltonians $H(\lambda)$ with response functions χ^λ,

$$\chi^\lambda(\boldsymbol{r},\boldsymbol{r}',\omega) = \frac{\delta n(\boldsymbol{r},\omega)}{\delta v_\lambda(\boldsymbol{r}',\omega)}. \tag{108}$$

The states Ψ_j form a complete basis set, so that

$$\sum_{j=0}^{\infty} |\Psi_j\rangle \langle\Psi_j| = \mathbb{1} \tag{109}$$

which can be used to rewrite equation (107) to

$$\int_0^\infty d\omega\, \chi(\boldsymbol{r},\boldsymbol{r}',\mathrm{i}\,\omega) + \chi(\boldsymbol{r},\boldsymbol{r}',\mathrm{i}\,\omega) =$$

$$-\pi\Big(\langle\Psi_0|\hat{n}(\boldsymbol{r})\hat{n}(\boldsymbol{r}')|\Psi_0\rangle + \langle\Psi_0|\hat{n}(\boldsymbol{r}')\hat{n}(\boldsymbol{r})|\Psi_0\rangle - 2\,\langle\Psi_0|\hat{n}(\boldsymbol{r})|\Psi_0\rangle\,\langle\Psi_0|\hat{n}(\boldsymbol{r}')|\Psi_0\rangle \Big) \tag{110}$$

and after rearranging the terms and renaming the ground state Ψ_0 to $\Psi(\lambda)$

$$\langle\Psi(\lambda)|\frac{\hat{n}(\boldsymbol{r})\hat{n}(\boldsymbol{r}') + \hat{n}(\boldsymbol{r}')\hat{n}(\boldsymbol{r})}{2}|\Psi(\lambda)\rangle =$$

$$-\frac{1}{\pi}\int_0^\infty \frac{\chi^\lambda(\boldsymbol{r},\boldsymbol{r}',\mathrm{i}\,\omega) + \chi^\lambda(\boldsymbol{r},\boldsymbol{r}',\mathrm{i}\,\omega)}{2}\, d\omega + n(\boldsymbol{r})n(\boldsymbol{r}') \tag{111}$$

where $n(\boldsymbol{r})$ and $n(\boldsymbol{r}')$ is the ground state density, which is supposed to be constant for all λ. Inserting this in equation (99) one obtains

$$E_{\mathrm{Hxc}} = \frac{1}{2}\int_0^1 d\lambda \int d^3\boldsymbol{r} d^3\boldsymbol{r}' \frac{1}{|\boldsymbol{r}-\boldsymbol{r}'|}\times$$

$$\times\left(-\frac{1}{\pi}\int_0^\infty \frac{\chi^\lambda(\boldsymbol{r},\boldsymbol{r}',\mathrm{i}\,\omega) + \chi^\lambda(\boldsymbol{r}',\boldsymbol{r},\mathrm{i}\,\omega)}{2}\, d\omega + n(\boldsymbol{r})n(\boldsymbol{r}') - \delta^{(3)}(\boldsymbol{r}-\boldsymbol{r}')n(\boldsymbol{r})\right) \tag{112}$$

$$= \frac{1}{2}\int_0^1 d\lambda \int d^3\boldsymbol{r} d^3\boldsymbol{r}' \frac{1}{|\boldsymbol{r}-\boldsymbol{r}'|}\left(-\frac{1}{\pi}\int_0^\infty \chi^\lambda(\boldsymbol{r},\boldsymbol{r}',\mathrm{i}\,\omega)\, d\omega + n(\boldsymbol{r})n(\boldsymbol{r}') - \delta^{(3)}(\boldsymbol{r}-\boldsymbol{r}')n(\boldsymbol{r})\right). \tag{113}$$

From equation (112) to equation (113), the integration variables were interchanged for the $\chi^\lambda(\boldsymbol{r}',\boldsymbol{r},\mathrm{i}\,\omega)$-term and the order of integration was then reversed again, in a similar

manner as described after equation (99). If the Hartree term

$$E_{\rm H} = \frac{1}{2}\int d^3\boldsymbol{r}d^3\boldsymbol{r}'\frac{1}{|\boldsymbol{r}-\boldsymbol{r}'|}n(\boldsymbol{r})n(\boldsymbol{r}') \tag{114}$$

is subtracted from equation (113) one finally obtains

$$\begin{aligned} E_{\rm xc} &= E_{\rm Hxc} - E_{\rm H} \\ &= -\frac{1}{2}\int_0^1 d\lambda \int d^3\boldsymbol{r}d^3\boldsymbol{r}'\frac{1}{|\boldsymbol{r}-\boldsymbol{r}'|}\left(\frac{1}{\pi}\int_0^\infty \chi^\lambda(\boldsymbol{r},\boldsymbol{r}',{\rm i}\,\omega)\,d\omega + \delta^{(3)}(\boldsymbol{r}-\boldsymbol{r}')n(\boldsymbol{r})\right), \end{aligned} \tag{115}$$

which is the result stated in equation (35). It will now be shown, that

$$-\frac{1}{2}\int d^3\boldsymbol{r}d^3\boldsymbol{r}'\frac{\delta^{(3)}(\boldsymbol{r}-\boldsymbol{r}')n(\boldsymbol{r})}{|\boldsymbol{r}-\boldsymbol{r}'|} = E_{\rm EXX} + \frac{1}{2}\int d^3\boldsymbol{r}d^3\boldsymbol{r}'\frac{1}{\pi}\int_0^\infty d\omega\frac{\chi^0(\boldsymbol{r},\boldsymbol{r}',{\rm i}\,\omega)}{|\boldsymbol{r}-\boldsymbol{r}'|} \tag{116}$$

which can be used in order to obtain a compact form for the correlation energy $E_{\rm c} = E_{\rm xc} - E_{\rm x}^{\rm KS}$ in terms of response functions only.

If equations (87) and (88) are used in conjunction with (107), then

$$\int d^3\boldsymbol{r}d^3\boldsymbol{r}'\int_0^\infty d\omega\frac{1}{\pi}\int_0^\infty \frac{\chi^0(\boldsymbol{r},\boldsymbol{r}',{\rm i}\,\omega)}{|\boldsymbol{r}-\boldsymbol{r}'|} = -\int d^3\boldsymbol{r}d^3\boldsymbol{r}'\sum_{\substack{n\in uocc\\ m\in occ}}\frac{\phi_n(\boldsymbol{r})\phi_m^*(\boldsymbol{r})\phi_n^*(\boldsymbol{r}')\phi_m(\boldsymbol{r}')}{|\boldsymbol{r}-\boldsymbol{r}'|}, \tag{117}$$

where the ϕ's are the Kohn-Sham orbitals since χ^0 is the Kohn-Sham response function. The Kohn-Sham exact exchange energy is given by [6]

$$E_{\rm EXX} = -\frac{1}{2}\int d^3\boldsymbol{r}d^3\boldsymbol{r}'\sum_{\substack{n\in occ\\ m\in occ}}\frac{\phi_n(\boldsymbol{r})\phi_n^*(\boldsymbol{r}')\phi_m(\boldsymbol{r}')\phi_m^*(\boldsymbol{r})}{|\boldsymbol{r}-\boldsymbol{r}'|}. \tag{118}$$

Adding together equation (117) and (118)

$$2E_{\mathrm{EXX}} + \int d^3\boldsymbol{r} d^3\boldsymbol{r}' \frac{1}{\pi} \int_0^\infty d\omega \frac{\chi^0(\boldsymbol{r}, \boldsymbol{r}', \mathrm{i}\,\omega)}{|\boldsymbol{r} - \boldsymbol{r}'|} =$$

$$- \left(\int d^3\boldsymbol{r} d^3\boldsymbol{r}' \sum_{\substack{n\in\mathrm{occ} \\ m\in\mathrm{occ}}} \frac{\phi_n(\boldsymbol{r})\phi_n^*(\boldsymbol{r}')\phi_m(\boldsymbol{r}')\phi_m^*(\boldsymbol{r})}{|\boldsymbol{r} - \boldsymbol{r}'|} + \sum_{\substack{n\in\mathrm{uocc} \\ m\in\mathrm{occ}}} \frac{\phi_n(\boldsymbol{r})\phi_m^*(\boldsymbol{r})\phi_n^*(\boldsymbol{r}')\phi_m(\boldsymbol{r}')}{|\boldsymbol{r} - \boldsymbol{r}'|} \right) \tag{119}$$

$$= - \int d^3\boldsymbol{r} d^3\boldsymbol{r}' \sum_{\substack{n \\ m\in\mathrm{occ}}} \frac{\phi_n(\boldsymbol{r})\phi_n^*(\boldsymbol{r}')\phi_m(\boldsymbol{r}')\phi_m^*(\boldsymbol{r})}{|\boldsymbol{r} - \boldsymbol{r}'|} \tag{120}$$

$$= - \int d^3\boldsymbol{r} d^3\boldsymbol{r}' \frac{1}{|\boldsymbol{r} - \boldsymbol{r}'|} \sum_n \phi_n(\boldsymbol{r})\phi_n^*(\boldsymbol{r}') \sum_{m\in\mathrm{occ}} \phi_m(\boldsymbol{r}')\phi_m^*(\boldsymbol{r}) \tag{121}$$

$$= - \int d^3\boldsymbol{r} d^3\boldsymbol{r}' \frac{\delta^{(3)}(\boldsymbol{r} - \boldsymbol{r}')n(\boldsymbol{r})}{|\boldsymbol{r} - \boldsymbol{r}'|} \tag{122}$$

where from equation (121) to (122) the fact that the ϕ_n form an orthonormal basis was used as well as equation (30) for the density of the Kohn-Sham system. Finally, after combining (122) with (115), the correlation energy $E_{\mathrm{c}} = E_{\mathrm{xc}} - E_{\mathrm{x}}^{\mathrm{KS}}$ reads

$$E_{\mathrm{c}} = -\frac{1}{2} \int_0^1 d\lambda \int d^3\boldsymbol{r} d^3\boldsymbol{r}' \frac{1}{|\boldsymbol{r} - \boldsymbol{r}'|} \left(\frac{1}{\pi} \int_0^\infty \chi^\lambda(\boldsymbol{r}, \boldsymbol{r}', \mathrm{i}\,\omega) - \chi^0(\boldsymbol{r}, \boldsymbol{r}', \mathrm{i}\,\omega)\, d\omega \right) \tag{123}$$

$$= -\frac{1}{2\pi} \int_0^1 d\lambda \int_0^\infty d\omega\, \mathrm{Tr}\left\{ \left(\chi^\lambda(\mathrm{i}\,\omega) - \chi^0(\mathrm{i}\,\omega) \right) \mathrm{v} \right\}. \tag{124}$$

$$= -\frac{1}{\pi} \int_0^1 d\lambda \int_{-\infty}^\infty d\omega\, \mathrm{Tr}\left\{ \left(\chi^\lambda(\mathrm{i}\,\omega) - \chi^0(\mathrm{i}\,\omega) \right) \mathrm{v} \right\}. \tag{125}$$

where v is the Coulomb kernel, which is in real space just

$$\mathrm{v}(\boldsymbol{r}, \boldsymbol{r}') = \frac{1}{|\boldsymbol{r} - \boldsymbol{r}'|}. \tag{126}$$

The extension of the ω-integration can be verified by looking at equation (106), giving another factor of $\frac{1}{2}$.

3.2 ACFDT-RPA

In the ACFDT-RPA, χ^λ is approximated in a certain way, that the λ-integration can be circumvented. The independent particle polarizabilty and the full polarizability are connected through the Dyson equation

$$\chi(\boldsymbol{r},\boldsymbol{r}',\omega) = \chi^0(\boldsymbol{r},\boldsymbol{r}',\omega) + \int d\boldsymbol{r}''d\boldsymbol{r}'''\chi^0(\boldsymbol{r},\boldsymbol{r}'',\omega)\left(\mathrm{v}(\boldsymbol{r}'',\boldsymbol{r}''') + K_{\mathrm{xc}}(\boldsymbol{r}'',\boldsymbol{r}''')\right)\chi(\boldsymbol{r}''',r',\omega) \tag{127}$$

as shown in reference [18]. In equation (127), K_{xc} is the exchange-correlation kernel defined as

$$K_{\mathrm{xc}}(\boldsymbol{r},\boldsymbol{r}') = \frac{\delta^2 E_{\mathrm{xc}}}{\delta n(\boldsymbol{r})\delta n(\boldsymbol{r}')}. \tag{128}$$

Equation (127) can be easily modified to account for the polarizability χ^λ of the system with an attenuated Coulomb interaction, leading to

$$\begin{aligned}\chi^\lambda(\boldsymbol{r},\boldsymbol{r}',\omega) =& \chi^0(\boldsymbol{r},\boldsymbol{r}',\omega) + \\ &+ \int d\boldsymbol{r}''d\boldsymbol{r}'''\chi^0(\boldsymbol{r},\boldsymbol{r}'',\omega)\left(\lambda\,\mathrm{v}(\boldsymbol{r}'',\boldsymbol{r}''') + K^\lambda_{\mathrm{xc}}(\boldsymbol{r}'',\boldsymbol{r}''')\right)\chi^\lambda(\boldsymbol{r}''',r',\omega)\end{aligned} \tag{129}$$

The random phase approximation neglects the influence of the exchange-correlation kernel by setting $K^\lambda_{\mathrm{xc}}(\boldsymbol{r},\boldsymbol{r}') = 0$, giving an approximate equation for the polarizability

$$\begin{aligned}\chi^\lambda(\boldsymbol{r},\boldsymbol{r}',\omega) \approx& \chi^{\lambda,\mathrm{RPA}}(\boldsymbol{r},\boldsymbol{r}',\omega) = \\ &\chi^0(\boldsymbol{r},\boldsymbol{r}',\omega) + \int d\boldsymbol{r}''d\boldsymbol{r}'''\chi^0(\boldsymbol{r},\boldsymbol{r}'',\omega)\lambda\,\mathrm{v}(\boldsymbol{r}'',\boldsymbol{r}''')\chi^{\lambda,\mathrm{RPA}}(\boldsymbol{r}''',r',\omega).\end{aligned} \tag{130}$$

Writing this in matrix notation

$$\chi^{\lambda,\mathrm{RPA}}(\omega) = \chi^0(\omega) + \lambda\chi^0(\omega)\,\mathrm{v}\,\chi^{\lambda,\mathrm{RPA}}(\omega) \tag{131}$$

$$(1-\lambda\chi^0(\omega)\,\mathrm{v})\chi^{\lambda,\mathrm{RPA}}(\omega) = \chi^0(\omega) \tag{132}$$

$$\chi^{\lambda,\mathrm{RPA}}(\omega) = (1-\lambda\chi^0(\omega)\,\mathrm{v})^{-1}\chi^0(\omega) \tag{133}$$

Using this in equation (124) yields

$$E_{\mathrm{c}}^{\mathrm{RPA}} = -\frac{1}{2\pi}\int_0^1 d\lambda \int_0^\infty d\omega\,\mathrm{Tr}\left\{(1-\lambda\chi^0(\mathrm{i}\,\omega)\,\mathrm{v})^{-1}\chi^0(\mathrm{i}\,\omega)\,\mathrm{v} - \chi^0(\mathrm{i}\,\omega)\,\mathrm{v}\right\} \tag{134}$$

By replacing

$$\mathrm{Tr}\left\{(1-\lambda\chi^0(\omega)\,\mathrm{v})^{-1}\chi^0(\omega)\,\mathrm{v}\right\} = -\frac{\partial}{\partial\lambda}\,\mathrm{Tr}\left\{\ln(1-\lambda\chi^0(\omega)\,\mathrm{v})\right\} \tag{135}$$

we finally get

$$E_{\mathrm{c}}^{\mathrm{RPA}} = \frac{1}{2\pi}\int_0^\infty d\omega\,\mathrm{Tr}\left\{\ln(1-\chi^0(\mathrm{i}\,\omega)\,\mathrm{v}) + \chi^0(\mathrm{i}\,\omega)\,\mathrm{v}\right\}. \tag{136}$$

4 Calculating intermolecular binding energies with an RPA algorithm

The Vienna *ab initio* simulation package (VASP) employs an implementation of the RPA algorithm presented in [1]. The calculation of the correlation energy E_c in this implementation was tested for different non-covalent complexes consisting of two molecules. The complexes were chosen from the S22 test set. The geometries were taken from *BEGDB* [19],[20],[21]. The complexes investigated in this thesis are listed in the following table:

Table 1: *Selected complexes from the S22 test set*

system name	molecular formular	S22-Refernce number
ammonia dimer	$(NH_3)_2$	1
water dimer	$(H_2O)_2$	2
formic acid dimer	$(HCOOH)_2$	3
formamide dimer	$(HCONH_2)_2$	4
methane dimer	$(CH_4)_2$	8
benzene dimer parallel displaced	$(C_6H_6)_2$	11
ethene ethyne complex	$C_2H_4 + C_2H_2$	16
benzene water complex	$C_6H_6 + H_2O$	17

VASP simulates systems with periodic boundary conditions. Usually a unit cell is defined and the program calculates the energy/unit cell for a periodically continued lattice. This gives the desired results for crystal structures, were finite size effects are neglected. However in this thesis, we were only interested in the binding energy between two molecules in vacuum. In order to calculate the binding energy of single complexes in VASP, as listed in table (1), a procedure to calculate the Hartree-Fock energy and the RPA correlation energy was followed for different unit cell volumes V until they converged. The results were extrapolated to $V \to \infty$ in order to remove finite size effects from the calculations.

4.1 Procedure for calculating the Hartree-Fock and RPA correlation energy of a crystal in VASP

As mentioned above, VASP is designed for the simulation of systems with periodic boundary conditions such as crystals. Therefore the binding energy between two molecules is not directly accessible. However, one can calculate the energy per unit cell for a lattice, where each unit cell contains the molecules for which the binding energy should be determined. This energy per unit cell would be identical to the binding

energy of the two molecules in vacuum, if the interaction energy of the two-molecule-complex with the surrounding lattice could be neglected. This is indeed the case for very large unit cell volumes. Unfortunately the computational costs increase dramatically ($\propto V^3$) with the basis cell volume, limiting the possibilities of simply using very large basis cells.
This section contains the procedure that was used to calculate the energy (Hartree-Fock and RPA correlation) per unit cell for different systems with VASP. The simulated systems were always lattices, with only one molecular complex from table (1) lying in the primitive cell. How this is related to the calculation of the actual binding energy for the molecule complex in vacuum will be elaborated in the next section.

The latest gamma-point only version *vasp.5.3.5_gmpi* was used for all steps and PBE [10] orbitals were chosen for the DFT calculations of all different species that were simulated. In practice, this was done by using the PBE `POTCAR` files for all the involved atoms. The `POTCAR` file for a certain molecule was created by concatenating the `POTCAR` files of the different atom types in the molecule into one file. The `POSCAR` files, which determine the geometry of the system, were set up as tetragonal cells, containing either the molecule or complex of interest with the geometry taken from `BEGDB`. The `KPOINTS` file determines for which k-points the energies will be calculated. Since we were only interested in binding energies between two molecules, the `KPOINTS` file was set up with the gamma point only. After the `POTCAR, POSCAR` and `KPOINTS` files where set up correctly the energy per unit cell was calculated in four steps. What follows is an operating procedure for those four steps [22],[23].

In each step, the `INCAR` file contains different flags and parameters that specify the tasks performed when VASP is executed. The flags used in the first step remain in all following steps, if it is not explicitly stated otherwise. To accelerate the computations, the `NCORE` flag can be set according to the recommendations in the manual [23]. In the context of this thesis this was `NCORE=4`, distributing one orbital one four cores. In the first step, the occupied orbitals of the DFT Hamiltonian are calculated. Gaussian smearing with a width of 0.05 eV is used for the partial occupancies, indicated by `ISMEAR=0` and `SIGMA=0.05` in the `INCAR` file. Additionally the global break-condition for the self consistency loops is specified by the energy difference between two consecutive steps, which is chosen to be 10^{-8} eV by using the flag `EDIFF=1.E-8`. It is important to keep the `OUTCAR` file, since it contains important information for the third step.

In the second step the Hartree-Fock energy is calculated non self-consistently from the DFT orbitals calculated in the first step. To tell VASP that it should perform Hartree-Fock/DFT hybrid functional type calculations, one has to set `LHFCALC=.TRUE.`. The flag `NELM=1` sets the number of electronic self-consistency steps to one, since they DFT

orbitals are already calculated. `AEXX=1` specifies that the whole exact exchange energy accounts for the energy and no averaging with LDA exchange energy is performed. In order to allow to recalculate one electron energies and perform selected postprocessing using the current orbitals specified in the `WAVECAR` file, `ALGO=Eigenval` was set. To prevent the program from overwriting the orbitals calculated in step one, the flag `LWAVE = .FALSE.` is used. After applying these changes to the `INCAR` file, VASP can be executed again and the Hartree-Fock energy calculated using the original DFT orbitals can be found in the `OUTCAR` file as total energy ("TOTEN").

In the third step, all virtual states are calculated by an exact diagonalization of the DFT Hamiltonian, specified by setting `ALGO=Exact` in the `INCAR` file. For this calculation, one has to look up the "maximum number of plane waves" in the `OUTCAR` file from the first step. This number is multiplied by two, if a gamma point only version is used, as this is the case in this thesis. The `NBANDS` flag is then set to the next higher number that is a multiple of the number of cores used for the computation. For example, if 32 cores are used for the computation and the "maximum of number of plane waves" is 500, one would set `NBANDS=1024`. `NELM=1` is used like it was in step two. Additionally `LOPTICS=.TRUE.` is used to calculate the frequency dependent dielectric matrix [22]. After VASP is executed again with this settings, everything is ready to calculate the RPA correlation energy in the fourth step.

In this final step, the `NCORE` flag is not enhancing the performance and is therefore set to its default value `NCORE=1`. `ALGO=RPAR` specifies the RPA algorithm developed in [1], which was used throughout this thesis for the calculation of the correlation energy. `NOMEGA` determines the grid used for the Fourier transforms between imaginary time and imaginary frequency domains. In this thesis we used `NOMEGA=8`. The basis of this calculation is equation 136, which reads in momentum space

$$E_{\mathrm{C}}^{\mathrm{RPA}} = \frac{1}{2\pi}\int_0^\infty d\omega \sum_{\boldsymbol{q}\in BZ}\sum_{\boldsymbol{G}} \ln\left(1-\chi^0(\boldsymbol{q},\mathrm{i}\,\omega)\,\mathrm{v}(\boldsymbol{q})\right)_{\boldsymbol{G},\boldsymbol{G}} + \chi^0(\boldsymbol{q},\mathrm{i}\,\omega)_{\boldsymbol{G},\boldsymbol{G}}\,\mathrm{v}(\boldsymbol{q})_{\boldsymbol{G},\boldsymbol{G}}. \quad (137)$$

In VASP, the sum over $\boldsymbol{G}$ is truncated at a certain $\boldsymbol{G}_{\max}$ determined by the $ENCUTGW$ flag in the following way

$$\frac{\hbar|\boldsymbol{q}+\boldsymbol{G}|^2}{2m_{\mathrm{e}}} < ENCUTGW. \quad (138)$$

VASP automatically extrapolates the RPA correlation energy by applying a linear regression of the form [24],[25]

$$E_{\mathrm{C}}^{\mathrm{RPA}}(\boldsymbol{G}) = E_{\mathrm{C}}^{\mathrm{RPA}}(\infty) + \frac{A}{\boldsymbol{G}^3} \quad (139)$$

to the calculated data. After VASP is executed in this step, the converged value of $E_{\mathrm{C}}^{\mathrm{RPA}}$ from the linear regression is found in the OUTCAR file (third string in the line that starts with string "converged").

After all steps are performed one has the Hartree-Fock as well as the RPA correlation energy per unit cell of the observed system.

4.2 Converging the two-molecule binding energy

The method described above is used to calculate the energy per unit cell for periodic boundary conditions. Since we are interest in the binding energy of two molecules only, one should theoretically use an infinitely extended unit cell, in order to eliminate the interactions due to the periodic boundary conditions. In practice, the unit cell volume has to be chosen finite, but should be sufficiently large so that the interactions from the periodically repeated images of the molecules in the primitive cell can be neglected. However the computational cost increases dramatically with unit cell size. Therefore it is useful to calculate the energies for different unit cell sizes and to extrapolate the results to infinite unit cell volumes.

In order to calculate the binding energy, we performed three calculations. In the first two steps the energy per unit cell of each single molecule that make up the complex was calculated. In the third step the energy per unit cell of the complex was calculated. The difference between the sum of the single molecule energies and the complex was extrapolated to yield the binding energy ΔE:

$$\Delta E = E_{\text{complex}} - (E_{\text{molecule 1}} + E_{\text{molecule 2}}). \tag{140}$$

Also in the case of dimers, the energy for both single molecules, even though they are chemically identical, was simulated individually since the different geometry, i.e. positions in the unit cell could lead to different results due to the periodic boundary conditions. The error that is not accounted for is the interaction between molecule 1 with the periodic copies of molecule 2 and vice versa. This error is the main reason why we have to increase the unit cell volume V and extrapolate to $V \to \infty$ where the error should vanish. This circumstances are illustrated in Fig. 1. Since we considered electrically neutral molecules the dominant term contributing to the error in the Hartree-Fock energy is the dipole-dipole interaction, that is in real space $\propto \frac{1}{\boldsymbol{r}^3} \propto \frac{1}{V}$. Hence it was expected that the error in the Hartree-Fock part of the binding energy would decrease with $\frac{1}{V}$ and that the converged Hartree-Fock binding energy $\Delta E_{HF}(\infty)$

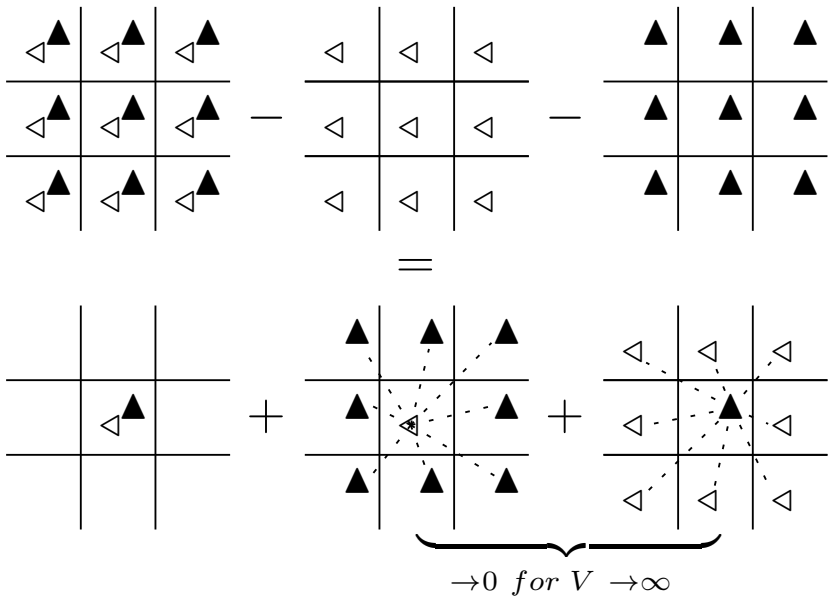

Figure 1: *Illustration of the calculation procedure for determining the binding energy between two molecules in VASP. The triangles symbolize molecules with different orientations in the unit cell. In each of the terms on the top, all of the molecules interact with each other. However on the bottom, only molecules of different type are meant to interact with each other, indicated by the dashed lines.*

can be calculated by a linear regression of the form

$$\Delta E_{\mathrm{HF}}(V) = k \cdot \frac{1}{V} + \Delta E_{\mathrm{HF}}(\infty). \tag{141}$$

For the correlation part of the binding energy $\Delta E_{\mathrm{C}}^{\mathrm{RPA}}$ we expected that the error would decrease with $\frac{1}{r^6} \propto \frac{1}{V^2}$ which is the typical van-der-Waals behaviour. The data was fitted with a three parameter function

$$\Delta E_{\mathrm{C}}^{\mathrm{RPA}}(V) = \Delta E_{\mathrm{C}}^{\mathrm{RPA}}(\infty) - \frac{k}{(V - V_0)^2} \tag{142}$$

where V_0 is an additional parameter, physically motivated by the picture of a volume associated with the two molecules.

4.3 Results for the binding energies and their convergence

In this subsection, "complex XX" refers to the S-22 reference number from table (1). The Hartree-Fock binding energy showed the expected $\frac{1}{V}$ behaviour. The limiting convergence behaviour was observed at cell volumes at around 1500 Å^3 for the small complexes like 1,2 and 8 and at around 2000 Å^3 for the larger complexes like 11 and

17. Also the chemical properties of the complexes influenced the convergence of the HF binding energy. Molecules with hydroxyl and carbonyl groups needed larger cell volumes to reach convergence because of their asymmetrical polar bonds and the resulting strong net dipole momentum, causing stronger long range interactions. The convergence of the Hartree-Fock energies is shown in Fig.2. Note that Fig. 2 only shows the energy relative to the converged values. The absolute converged values are presented in table (2).

For RPA correlation energies, the convergence was reached quicker, however the computation time was exceeding the HF-calculations by far, also for volumes below 1000 Å^3. For this reason we focused on certain complexes and chose to investigate $1, 2, 3$ and 17 in more detail. For each of these four complexes, up to 20 simulations at different unit cell volumes ranging from 100-1150 Å^3 were performed. In the case of 17, we even went to larger volumes, with a maximum at 1500 Å^3. The RPA correlation energies for complexes $4, 8, 11$ and 16 were calculated at only four to six different volumes ranging from 100-1000 Å^3. The results are presented in two figures, Fig. 3 and Fig. 4, where the first one summarizes the results of all investigated complexes and the later shows the results for the selected complexes in more detail.

For small volumes it was observed that $\Delta E_{\mathrm{c}}^{\mathrm{RPA}}$ converged even faster then $\frac{1}{V^2}$, *e.g.* $\frac{1}{V^3}$. For this reason, the van der Waals energies were calculated by employing the *DFT-D2 method of Grimme* [3], which was carried out by setting the flag `LVDW=.TRUE.` in the INCAR files. The aim was to find out if the vdW energies also show this behaviour. At least for large volumes the *DFT-D2 method of Grimme* [3] should show a $\frac{1}{V^2}$ convergence as it is set up with effective pair-potentials $\propto \frac{1}{|\boldsymbol{r}_i - \boldsymbol{r}_j|^6}$. In the case it did not show this behaviour for small volumes, it is reasonable to assume that the effect must be due to some geometric finite size effects and that the same applies to the behaviour of $\Delta E_{\mathrm{c}}^{\mathrm{RPA}}$. In fact this was the case, however, it was also found that if the fitting area was restricted to larger volumes, the $\frac{1}{V^2}$ fit indicated in equation (142) was in very good agreement with the observed data. The results obtained from the simulations with the *DFT-D2 method of Grimme* are represented in Fig. 5.

Finally it was investigated if an increase in the cut-off energy for the plane wave basis set of the orbitals has an effect on the convergence. This was only done for complexes 2 and 17 as it was a major computational effort. As shown in Fig. 6 and Fig. 7 , there was no significant improvement with increasing cut-off radius.

Table 2: *Converged energies in* [eV] *for selected complexes from the S22 test set*

S22 #	ΔE_{HF}	$\Delta E_{\mathrm{c}}^{\mathrm{RPA}}$	ΔE^{tot}	*lit.* ΔE^{tot} [4]	$\Delta E_{\mathrm{DFT}}^{\mathrm{tot}}$
1	-0.031	- 0.083	-0.114	-0.100	-0.117
2	-0.116	-0.070	-0.186	-0.165	-0.220
3	-0.554	-0.194	-0.748	-0.648	-0.780
4	-0.442	-0.204	-0.647	-0.557	-0.627
8	0.023	-0.034	-0.011	-0.013	-0.004
11	0.239	-0.338	-0.098	-0.059	0.082
16	-0.014	-0.048	-0.062	-0.040	-0.052
17	-0.023	-0.105	-0.137	-0.085	-0.084

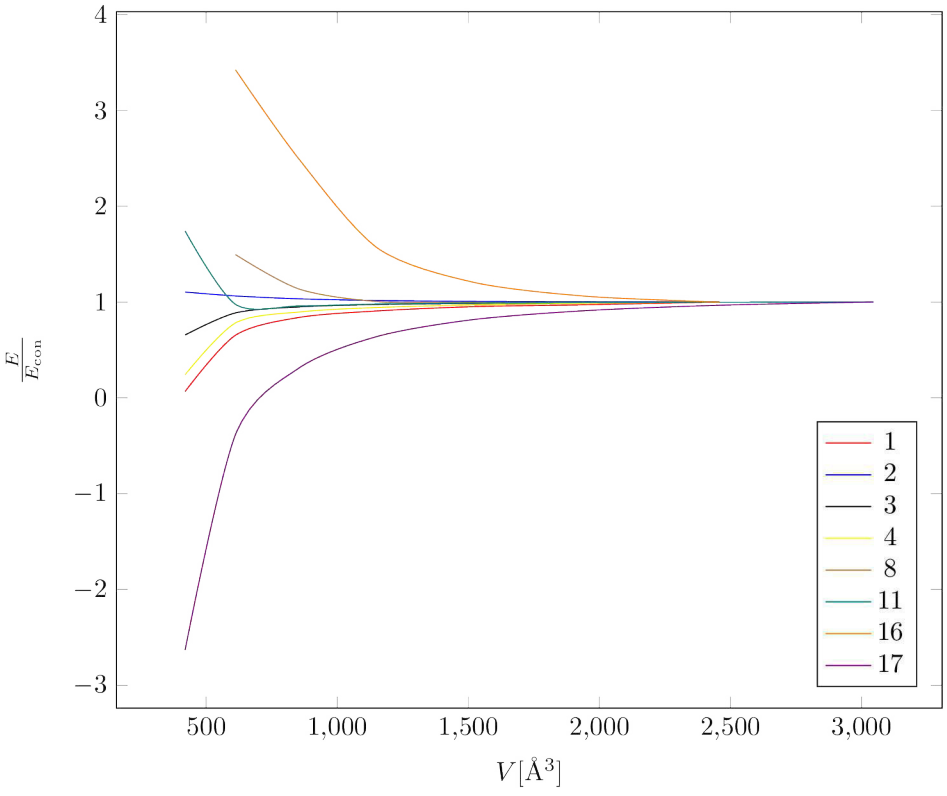

Figure 2: *Convergence of* E_{HF} *with increasing unit cell size.* $\frac{E}{E_{\mathrm{con}}}$ *is the ratio between the calculated energy at a certain unit cell volume and the converged value.*

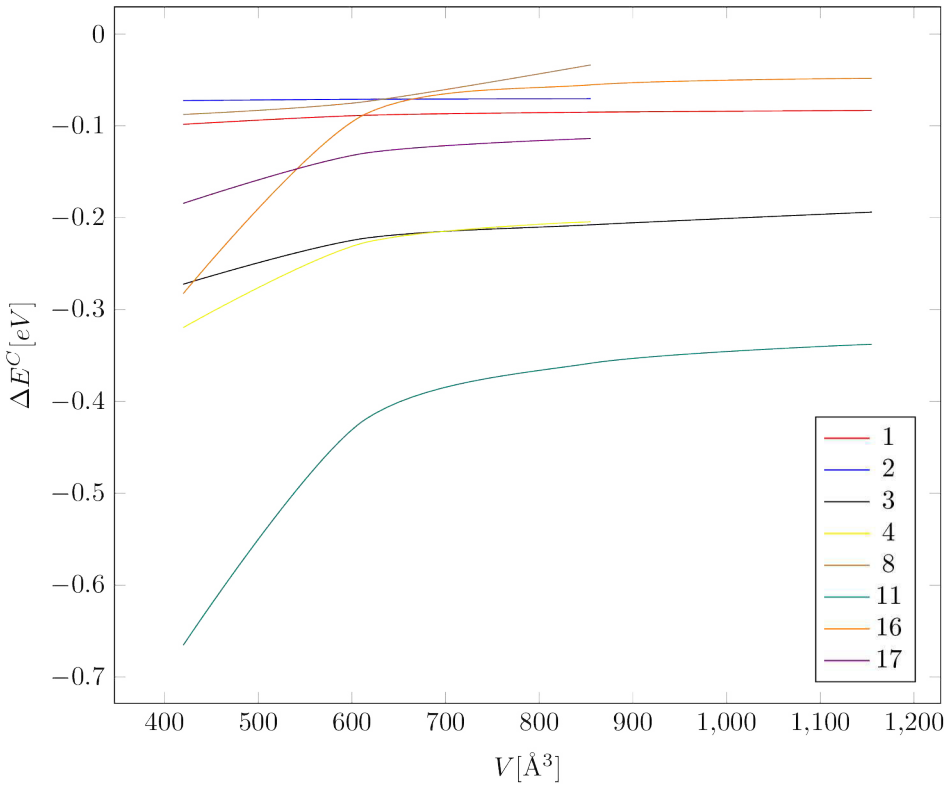

Figure 3: *Convergence of the RPA correlation energy with increasing unit cell size.*

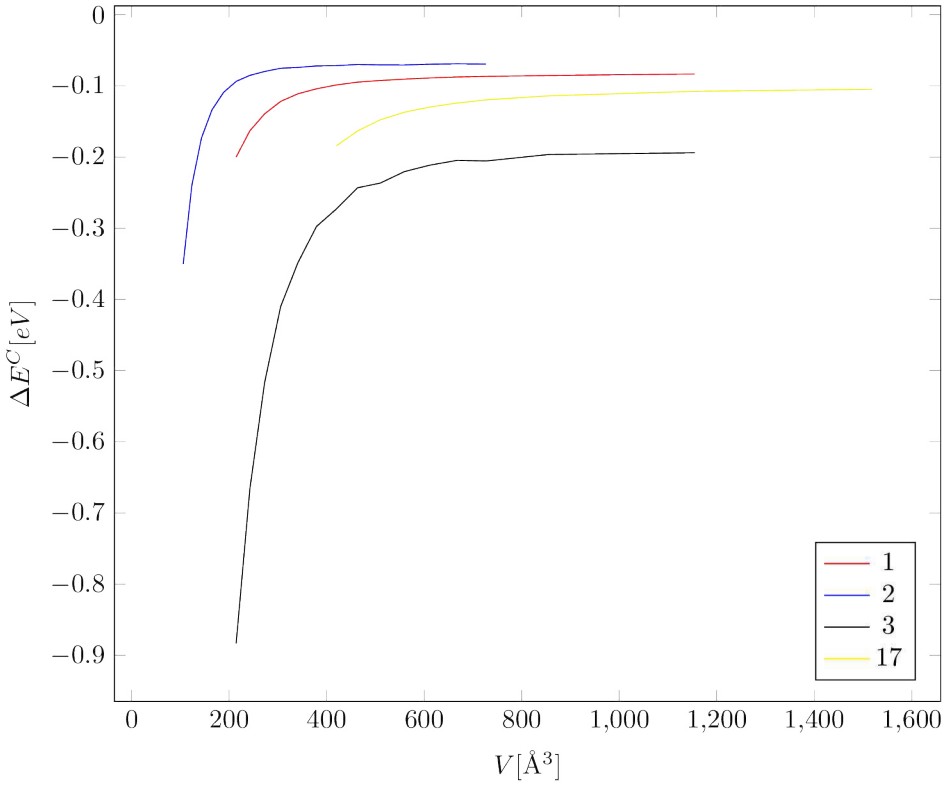

Figure 4: *Convergence of the RPA correlation energy with increasing unit cell size with more data points.*

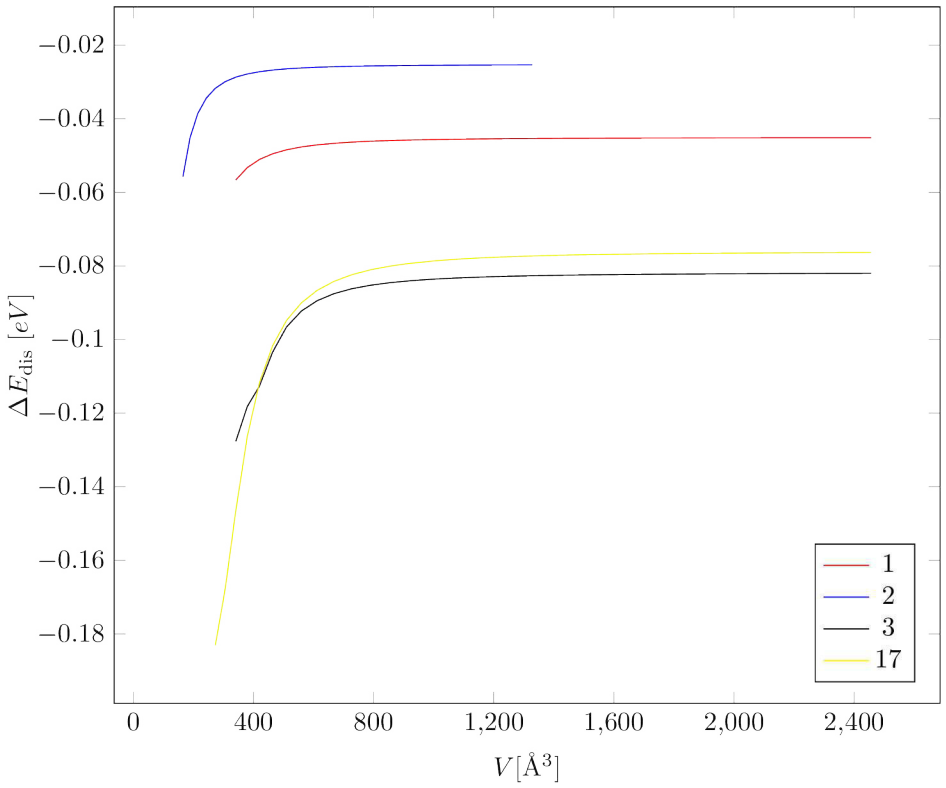

Figure 5: *Convergence of the vdW binding energy with increasing unit cell size using the DFT-D2 method of Grimme.*

[3]

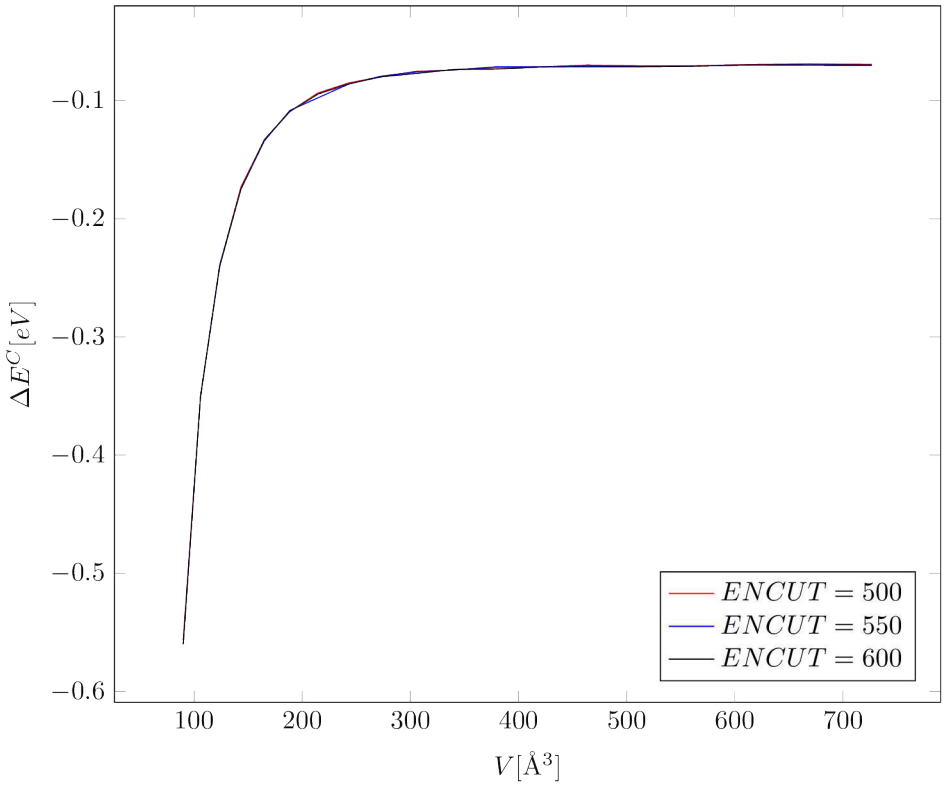

Figure 6: *Convergence of the RPA correlation energy for* 2 *with increasing unit cell size at different cut-off energies.*

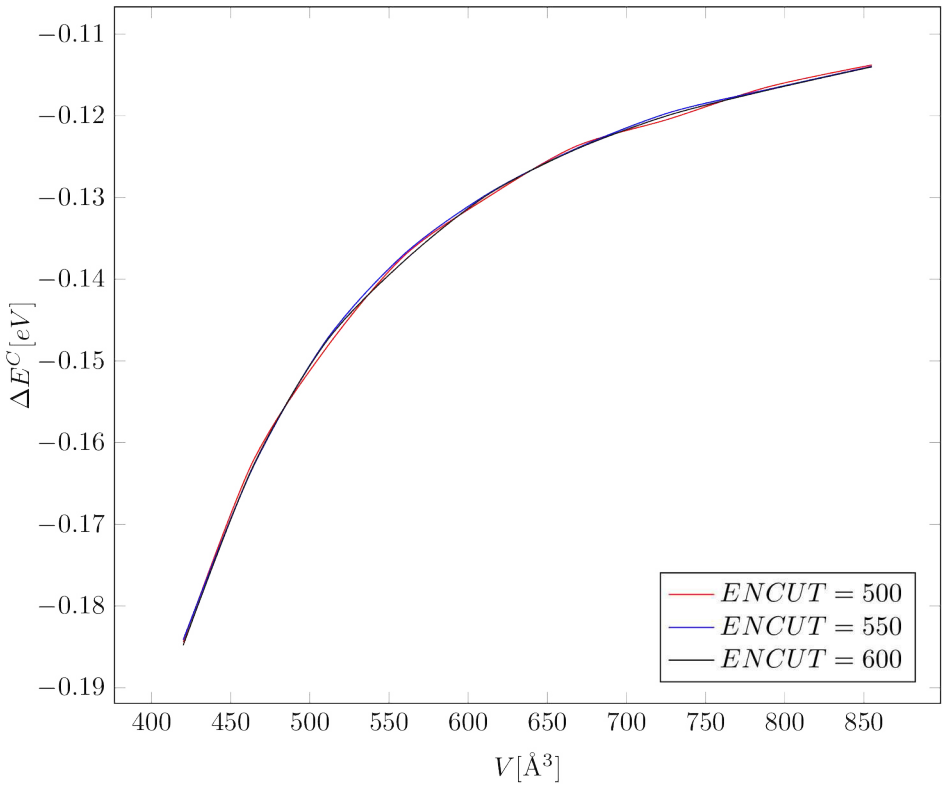

Figure 7: *Convergence of the RPA correlation energy for* 17 *with increasing unit cell size at different cut-off energies.*

5 The Green's function or propagator G

In this section the Green's functions will be introduced briefly. Later on in the following sections, the connection to the calculation of energy variations that lead to the calculation of forces will be established.

The evolution with time of a quantum system is described by the time dependent Schrödinger equation

$$(\mathrm{i}\,\frac{\partial}{\partial t} - H)\,|\Psi\rangle = 0. \tag{143}$$

The stationary Schrödinger equation, which is an eigenvalue equation for the Hamiltonian, is given by

$$H\,|\phi_n\rangle = \epsilon_n\,|\phi_n\rangle \quad n \in \mathbb{N}, \tag{144}$$

where the $|\phi_n\rangle$ are eigenstates of the unperturbed Hamiltonian H with eigenvalues ϵ_n. Given a quantum system in state $|\Psi(t_0)\rangle$, the propagation with time may be calculated formally by solving the Schrödinger equation (143)

$$|\Psi(t)\rangle = e^{-iH(t-t_0)}\,|\Psi(t_0)\rangle = \underbrace{\sum_n e^{-\,\mathrm{i}\,\epsilon_n(t-t_0)}\,|\phi_n\rangle\,\langle\phi_n}_{U(t,t_0)}\,|\Psi(t_0)\rangle\,. \tag{145}$$

In order to get a fundamental solution (i.e. Green's function) of the Schrödinger equation,

$$(\mathrm{i}\,\frac{\partial}{\partial t} - H)G(t,t_0) = \delta(t-t_0)\cdot\mathbb{1}, \tag{146}$$

it is useful to examine equation (145) in more detail. If the time evolution operator $U(t,t_0)$ acting on $\Psi(t_0)$ on the right hand side is multiplied by $\delta(t-t_0)$ it yields

$$\delta(t-t_0)\cdot\sum_n e^{-\,\mathrm{i}\,\epsilon_n(t-t_0)}\,|\phi_n\rangle\,\langle\phi_n| = \delta(t-t_0)\cdot\mathbb{1}, \tag{147}$$

where the fact that ϕ_n form a complete orthonormal basis set was used. This is exactly the desired result when the Green's function is put into the Schrödinger equation. On the other hand

$$(\mathrm{i}\,\frac{\partial}{\partial t} - H)U(t,t_0) = 0. \tag{148}$$

Using the relation

$$\frac{\partial}{\partial t}\theta(t) = \delta(t) \tag{149}$$

and combining the observations from above one gets

$$(\mathrm{i}\,\frac{\partial}{\partial t} - H)\theta(t-t_0)U(t,t_0) = \mathrm{i}\,\delta(t-t_0)U(t,t_0) + \theta(t-t_0)\,\underbrace{(\mathrm{i}\,\frac{\partial}{\partial t} - H)U(t,t_0)}_{=0}\,. \tag{150}$$

For fermions, a particle cannot propagate in an already occupied state. Therefore the summation over the occupied states in equation (145) can be omitted. The particle propagator (or Green's function) $\mathrm{i}\,G_0^+$ is then given by the greater Green's function

$$\mathrm{i}\,G_0^+(t_2-t_1) = \theta(t_2-t_1)\sum_{a\in unocc} |\phi_a\rangle\,\langle\phi_a|\,e^{-\,\mathrm{i}\,\epsilon_a(t_2-t_1)}. \tag{151}$$

The index a runs only over unoccupied states (i.e. $\epsilon_a > \epsilon_\mathrm{F}$, ϵ_F being the Fermi level).

Usually in the calculation of the full propagator, which includes perturbations in the Hamiltonian, convolution integrals with respect to time appear. Therefore it is useful to calculate the Fourier transform of G_0^+, since those convolutions become simple multiplications in frequency space. In order to make this Fourier transform converging, we multiply G_0^+ by a factor $\exp(-\eta(t_2-t_1))$. In this factor, η is a positive infinitesimal such that for any relevant finite time difference $\exp(-\eta(t_2-t_1)) \approx 1$, but in the limit $(t_2-t_1) \to \infty$, $\exp(-\eta\cdot(t_2-t_1)) = 0$. This modification has no physical relevant effect, since only finite time differences are of interest. Now the Fourier transform of the modified G_0^+ can be easily calculated:

$$G_0^+(\omega) = \int_{-\infty}^{\infty} d(t_2-t_1)\; G_0^+(t_2-t_1)\,e^{\mathrm{i}\,\omega(t_2-t_1)} \tag{152}$$

$$= \int_{-\infty}^{\infty} d(t_2-t_1)\; -\mathrm{i}\,\theta(t_2-t1)\,e^{-\,\mathrm{i}\,\epsilon_n(t_2-t_1)}\,e^{\eta(t_2-t_1)}\,e^{\mathrm{i}\,\omega(t_2-t_1)} \tag{153}$$

$$= -\frac{e^{\mathrm{i}(\omega-\epsilon_n-\mathrm{i}\,\eta)(t_2-t_1)}}{\omega-\epsilon_n+\mathrm{i}\,\eta}\bigg|_0^\infty \tag{154}$$

$$= \frac{1}{\omega-\epsilon_n+\mathrm{i}\,\eta} \tag{155}$$

Hence,

$$G_0^+(\omega) = \sum_{a \in uocc} |\phi_a\rangle \langle\phi_a| \frac{1}{\omega - \epsilon_a + \mathrm{i}\,\eta}. \tag{156}$$

In the context of particle-hole formalism, similar calculations can be carried out for holes too. In contrast to particles, holes can only propagate below the Fermi level (one could regard all the states above the Fermi level being occupied by holes). The creation of a hole (removal of a particle) increases the total energy of the system by an amount equal to the binding energy of the removed particle. Therefore the energy associated with a hole is the negative energy of the corresponding particle. The resulting sign change in the exponent of equation (145) may be related to the time difference $(t_2 - t_1)$ instead. Thus the propagation of a hole has the same form as a particle propagation with reversed time ordering. Taking all this into account, the hole propagator is given by the lesser Green's function

$$-\mathrm{i}\, G_0^-(t_2 - t_1) = \theta(t_1 - t_2) \sum_{i \in occ} |\phi_i\rangle \langle\phi_i|\, e^{-\mathrm{i}\,\epsilon_i (t_2 - t_1)}, \tag{157}$$

which yields the following expression in frequency space:

$$G_0^-(\omega) = \sum_{i \in occ} |\phi_i\rangle \langle\phi_i| \frac{1}{\omega - \epsilon_i - \mathrm{i}\,\eta} \tag{158}$$

The total unperturbed propagator is the sum $G_0^+ + G_0^-$:

$$G_0(\omega) = \sum_n |\phi_n\rangle \langle\phi_n| \frac{1}{\omega - \epsilon_n + \mathrm{i}\,\eta\,\mathrm{sgn}(\epsilon_n - \epsilon_F)} \tag{159}$$

6 A comparison between the Green's function formalism and perturbation theory

In the following, it is shown that the Green's function formalism yields the same results as standard perturbation theory (PT) in a convenient manner. In a first step, the reduced 1-particle density matrix γ is calculated from the Green's function G_0. Comparing equation (159) with the expression of γ in the basis of energy eigenstates one may recognise the following (using the abbreviation $|i\rangle = |\phi_i\rangle$):

$$\gamma = \sum_{i \in occ} |i\rangle \langle i| = \sum_{i \in occ} \mathrm{Res}_{\epsilon_i} \left(\frac{|i\rangle \langle i|}{\omega - \epsilon_i} \right) \tag{160}$$

The right-hand side of equation (160) (multiplied by $2\pi\,\mathrm{i}$) equals a counter clockwise contour integral of $G_0(\omega)$, containing all poles in the upper plane. One possible integration path is to integrate over the whole real axis from $-\infty$ to ∞ and close the integral in the upper half plane with $|\omega| \to \infty$. In order to make the second part vanish, G_0 is multiplied with a convergence factor $\exp(-\,\mathrm{i}\,\tau\omega)$. This factor yields just 1 in the limit $\tau \to 0^-$, so that finally

$$\lim_{\tau \to 0^-} \frac{1}{2\pi\,\mathrm{i}} \int_{-\infty}^{\infty} d\omega\, G_0(\omega) e^{-\,\mathrm{i}\,\tau\omega} = \sum_{i \in occ} \mathrm{Res}_{\epsilon_i + \mathrm{i}\,\eta} \left(\frac{|i\rangle \langle i|}{\omega - \epsilon_i - \mathrm{i}\,\eta} \right) = \gamma. \tag{161}$$

Now consider a small (frequency independent) perturbation δV in the Hamiltonian. In first order the Green's function of the perturbed system is given by the first order term in the Dyson equation:

$$G(\omega) = G_0(\omega) + G_0(\omega) \delta V G_0(\omega) + \mathcal{O}(\delta V^2) \tag{162}$$

and

$$\delta G(\omega) = G_0(\omega) \delta V G_0(\omega) \tag{163}$$

In analogy to the calculation of the density matrix, one may now try to calculate the change of the density matrix $\delta\gamma$ in first order.

$$\delta\gamma = \lim_{\tau\to 0^-} \frac{1}{2\pi\,\mathrm{i}} \int_{-\infty}^{\infty} d\omega\, G_0(\omega)\,\delta V G_0(\omega) e^{-\mathrm{i}\,\tau\omega} \tag{164}$$

$$= \lim_{\tau\to 0^-} \frac{1}{2\pi\,\mathrm{i}} \int_{-\infty}^{\infty} d\omega \sum_{n,m} \frac{|n\rangle\langle n|}{\omega - \epsilon_n + \mathrm{i}\,\eta\,\mathrm{sgn}(\epsilon_n - \epsilon_F)} \delta V \frac{|m\rangle\langle m|}{\omega - \epsilon_m + \mathrm{i}\,\eta\,\mathrm{sgn}(\epsilon_m - \epsilon_F)} e^{-\mathrm{i}\,\tau\omega} \tag{165}$$

$$= \sum_{i\in occ,m} \mathrm{Res}_{\epsilon_i + \mathrm{i}\,\eta}\left(\frac{|i\rangle\langle i|}{\omega - \epsilon_i - \mathrm{i}\,\eta} \delta V \frac{|m\rangle\langle m|}{\omega - \epsilon_m + \mathrm{i}\,\eta\,\mathrm{sgn}(\epsilon_m - \epsilon_F)}\right) \tag{166}$$

$$+ \sum_{i\in occ,n} \mathrm{Res}_{\epsilon_i + \mathrm{i}\,\eta}\left(\frac{|n\rangle\langle n|}{\omega - \epsilon_n + \mathrm{i}\,\eta\,\mathrm{sgn}(\epsilon_n - \epsilon_F)} \delta V \frac{|i\rangle\langle i|}{\omega - \epsilon_i - \mathrm{i}\,\eta}\right)$$

$$= \sum_{i\in occ, n\neq i} \frac{|i\rangle\langle i|\,\delta V\,|n\rangle\langle n| + |n\rangle\langle n|\,\delta V\,|i\rangle\langle i|}{\epsilon_i - \epsilon_n} \tag{167}$$

From equation (165) to (166) the integral is calculated by closing the integral along a path in the upper half with vanishing contribution and evaluating the contour integration (Jordan's lemma). Afterwards the limit $\tau \to 0^-$ can be carried out immediately, as ω only assumes finite values from now on. In equation (166) the summands where $i = m$ (or n respectively) vanish as $\mathrm{Res}_0(\frac{1}{z^2}) = 0$. The expression in equation (167) is the same one would get with standard first-order perturbation theory.

7 Energy variations

In order to calculate the force acting on an object with coordinates $\boldsymbol{R}$ in a system whose total energy is a functional $E[V_{\text{ext}}]$ of some external potential V_{ext}, one may formally write

$$\vec{F} = -\vec{\nabla}_{\boldsymbol{R}} E = -\int \frac{\delta E}{\delta V_{\text{ext}}(\boldsymbol{r})} \vec{\nabla}_{\boldsymbol{R}} V_{\text{ext}}(\boldsymbol{r}) \mathrm{d}^3\boldsymbol{r} \tag{168}$$

In the case of the Kohn-Sham system, V_{ext} is simply replaced with V^{KS}. The quantity $\vec{\nabla}_{\boldsymbol{R}} V^{\text{KS}}(\boldsymbol{r})$ can be calculated rather easily at low computational complexity within the DFT framework, for example with finite steps or the Hellman-Feynman theorem, which relies on the fact that the energy is variational with respect to the one electron orbitals. However it will not be elaborated here how this is done in detail. The difficult part is to calculate the term $\frac{\delta E}{\delta V}$ in equation (168). For the RPA or for a calculation of the Hartree-Fock energy using DFT-orbitals, one cannot rely on the variational properties. Therefore the derivative of the functional with respect to the changes of the orbitals resulting from a change of V_{ext} must be included and analytically or numerically determined. Therefore the focus of this work lies on the calculation of the functional derivatives of different energy functionals with respect to an external potential. In the following we denote the external potential simply with V for the sake of a compact notation. However in the practical application when the external potential is the KS-potential, one should just replace V with V^{KS} for clarification.

7.1 Variation of the Hartree-Fock Energy with the Green's function method

The Green's function method may be applied to calculate the change in energy caused by changes in the potential. In the Hartree-Fock approximation the energy is estimated by the functional E_{HF}.

$$E_{\text{HF}} = E_{\text{kin}} + E_{\text{ext}} + E_{\text{H}} + E_{\text{x}} \tag{169}$$

$$E_{\text{kin}} = -\frac{1}{2}\int\limits_{\mathbb{R}^3} d^3\boldsymbol{r} d^3\boldsymbol{r}'\, \delta(\boldsymbol{r}-\boldsymbol{r}')\nabla^2_{\boldsymbol{r}'} n(\boldsymbol{r}',\boldsymbol{r}) \tag{170}$$

$$E_{\text{ext}} = -\sum_k \int\limits_{\mathbb{R}^3} d^3\boldsymbol{r}\, \frac{Z_k}{|\boldsymbol{r}-\boldsymbol{R}_k|} n(\boldsymbol{r}) \tag{171}$$

$$E_{\text{H}} = \frac{1}{2}\iint\limits_{\mathbb{R}^3\mathbb{R}^3} d^3\boldsymbol{r} d^3\boldsymbol{r}'\, \frac{n(\boldsymbol{r})n(\boldsymbol{r}')}{|\boldsymbol{r}-\boldsymbol{r}'|} \tag{172}$$

$$\tag{173}$$

$$E_{\text{x}} = -\frac{1}{2}\iint\limits_{\mathbb{R}^3\mathbb{R}^3} d^3\boldsymbol{r} d^3\boldsymbol{r}'\, \frac{n(\boldsymbol{r},\boldsymbol{r}')n(\boldsymbol{r}',\boldsymbol{r})}{|\boldsymbol{r}-\boldsymbol{r}'|} \tag{174}$$

$$\text{where} \quad n(\boldsymbol{r},\boldsymbol{r}') = \langle \boldsymbol{r}|\gamma|\boldsymbol{r}'\rangle \quad \text{and} \quad n(\boldsymbol{r}) = n(\boldsymbol{r},\boldsymbol{r}). \tag{175}$$

The first term E_{kin} is the kinetic energy, whilst the second term is the energy due to the cores with fixed coordinates $\boldsymbol{R}_k$ and charge Z_k. The third term E_{H} is the *Hartree* energy, originating from the Coulomb repulsion of the electrons. This term is corrected by the exchange energy E_{x}, which has no classical analogue. However, classically spoken, it is plausible that E_{H} alone would overestimate the energy as it includes the energy of an electron due to its own field, which has a singularity at the position of the electron.

Now the question is how the energy changes due to a variation in the density matrix caused by a small perturbation in the Hamiltonian that "generated" the orbitals corresponding to the density matrix

$$\gamma = \sum_{i\in occ} |i\rangle\langle i| \quad \text{with} \;\; H|i\rangle = \epsilon_i |i\rangle \tag{176}$$

We assume that the perturbation is local, $\langle \boldsymbol{r}|\delta V|\boldsymbol{r}'\rangle \propto \delta(\boldsymbol{r}-\boldsymbol{r}')$ and independent of frequency ω.

7.1.1 Variation of the Hartree energy E_{H}

The variation δE_{H} can be calculated from the variation of the density and the corresponding Green's functions respectively,

$$\delta E_{\mathrm{H}} = \frac{1}{2} \iint\limits_{\mathbb{R}^3\mathbb{R}^3} d^3\boldsymbol{r} d^3\boldsymbol{r}' \, \frac{\delta n(\boldsymbol{r}) n(\boldsymbol{r}') + (\boldsymbol{r} \leftrightarrow \boldsymbol{r}')}{|\boldsymbol{r} - \boldsymbol{r}'|} = \iint\limits_{\mathbb{R}^3\mathbb{R}^3} d^3\boldsymbol{r} d^3\boldsymbol{r}' \, \frac{\delta n(\boldsymbol{r}) n(\boldsymbol{r}')}{|\boldsymbol{r} - \boldsymbol{r}'|}. \tag{177}$$

The change of the density matrix can be obtained from equation (164) and (175) and is given by:

$$2\pi \,\mathrm{i}\; \delta n(\boldsymbol{r}, \boldsymbol{r}') = 2\pi \,\mathrm{i}\, \langle \boldsymbol{r} | \delta\gamma | \boldsymbol{r}' \rangle \tag{178}$$

$$= \iint\limits_{\mathbb{R}^3\mathbb{R}^3} d^3\boldsymbol{r}'' d^3\boldsymbol{r}''' \lim_{\tau \to 0^-} \int\limits_{-\infty}^{\infty} d\omega \, G_0(\boldsymbol{r}, \boldsymbol{r}'', \omega) \delta V(\boldsymbol{r}'', \boldsymbol{r}''') G_0(\boldsymbol{r}''', \boldsymbol{r}', \omega) e^{-\,\mathrm{i}\,\omega\tau} \tag{179}$$

$$= \int\limits_{\mathbb{R}^3} d^3\boldsymbol{r}'' \lim_{\tau \to 0^-} \int\limits_{-\infty}^{\infty} d\omega \, G_0(\boldsymbol{r}, \boldsymbol{r}'', \omega) \delta V(\boldsymbol{r}'') G_0(\boldsymbol{r}'', \boldsymbol{r}', \omega) e^{-\,\mathrm{i}\,\omega\tau}. \tag{180}$$

Setting $\boldsymbol{r} = \boldsymbol{r}'$ in equation (180) gives $\delta n(\boldsymbol{r})$ and inserting the change of the density matrix in equation (177) gives

$$2\pi \,\mathrm{i}\; \delta E_{\mathrm{H}} = \int\limits_{\mathbb{R}^3} d^3\boldsymbol{r}'' \lim_{\tau \to 0^-} \iint\limits_{\mathbb{R}^3\mathbb{R}^3} d^3\boldsymbol{r} d^3\boldsymbol{r}' \int\limits_{-\infty}^{\infty} d\omega \, \frac{G_0(\boldsymbol{r}'', \boldsymbol{r}, \omega) n(\boldsymbol{r}') G_0(\boldsymbol{r}, \boldsymbol{r}'', \omega)}{|\boldsymbol{r} - \boldsymbol{r}'|} e^{-\,\mathrm{i}\,\omega\tau} \delta V(\boldsymbol{r}'') \tag{181}$$

$$= \int\limits_{\mathbb{R}^3} d^3\boldsymbol{r}'' \lim_{\tau \to 0^-} \int\limits_{\mathbb{R}^3} d^3\boldsymbol{r} \int\limits_{-\infty}^{\infty} d\omega \, G_0(\boldsymbol{r}'', \boldsymbol{r}, \omega) V_{\mathrm{H}}(\boldsymbol{r}) G_0(\boldsymbol{r}, \boldsymbol{r}'', \omega) e^{-\,\mathrm{i}\,\omega\tau} \delta V(\boldsymbol{r}'') \tag{182}$$

where

$$V_{\mathrm{H}}(\boldsymbol{r}) = \int\limits_{\mathbb{R}^3} d^3\boldsymbol{r}' \frac{n(\boldsymbol{r}')}{|\boldsymbol{r} - \boldsymbol{r}'|} \tag{183}$$

$$\Rightarrow \frac{\delta E_{\mathrm{H}}}{\delta V(\boldsymbol{r}'')} = \frac{1}{2\pi \,\mathrm{i}} \lim_{\tau \to 0^-} \int\limits_{\mathbb{R}^3} d^3\boldsymbol{r} \int\limits_{-\infty}^{\infty} d\omega \, G_0(\boldsymbol{r}'', \boldsymbol{r}, \omega) V_{\mathrm{H}}(\boldsymbol{r}) G_0(\boldsymbol{r}, \boldsymbol{r}'', \omega) e^{-\,\mathrm{i}\,\omega\tau}. \tag{184}$$

In accordance with equations (164) to (167), the expression above (184) can be written in terms of the one electron orbitals as:

$$\frac{\delta E_{\mathrm{H}}}{\delta V(\boldsymbol{r}'')} = \langle \boldsymbol{r}'' | \sum_{i \in occ, n \neq i} \frac{|i\rangle \langle i| \, V_{\mathrm{H}} \, |n\rangle \langle n| + |n\rangle \langle n| \, V_{\mathrm{H}} \, |i\rangle \langle i|}{\epsilon_i - \epsilon_n} \, |\boldsymbol{r}''\rangle \,. \tag{185}$$

7.1.2 Variation of the exchange energy E_{x}

Similarly, the variation of the exchange energy δE_{x} is can be written as:

$$\delta E_{\mathrm{x}} = -\frac{1}{2}\iint\limits_{\mathbb{R}^3\mathbb{R}^3} d^3\boldsymbol{r}d^3\boldsymbol{r}'\frac{\delta n(\boldsymbol{r},\boldsymbol{r}')n(\boldsymbol{r}',\boldsymbol{r}) + n(\boldsymbol{r},\boldsymbol{r}')\delta n(\boldsymbol{r}',\boldsymbol{r})}{|\boldsymbol{r}-\boldsymbol{r}'|} \tag{186}$$

$$= -\iint\limits_{\mathbb{R}^3\mathbb{R}^3} d^3\boldsymbol{r}d^3\boldsymbol{r}'\frac{\delta n(\boldsymbol{r},\boldsymbol{r}')n(\boldsymbol{r}',\boldsymbol{r})}{|\boldsymbol{r}-\boldsymbol{r}'|} \tag{187}$$

Inserting equation (180) in equation (187) yields

$$-2\pi\,\mathrm{i}\;\delta E_{\mathrm{x}} =$$

$$\int\limits_{\mathbb{R}^3} d^3\boldsymbol{r}'' \lim_{\tau\to 0^-}\iint\limits_{\mathbb{R}^3\mathbb{R}^3} d^3\boldsymbol{r}d^3\boldsymbol{r}'\int\limits_{-\infty}^{\infty} d\omega\, G_0(\boldsymbol{r}'',\boldsymbol{r}',\omega)V_{\mathrm{x}}(\boldsymbol{r}',\boldsymbol{r})G_0(\boldsymbol{r},\boldsymbol{r}'',\omega)e^{-\mathrm{i}\omega\tau}\delta V(\boldsymbol{r}'') \tag{188}$$

with

$$V_x(\boldsymbol{r}',r) = \frac{n(\boldsymbol{r}',\boldsymbol{r})}{|\boldsymbol{r}-\boldsymbol{r}'|} \tag{189}$$

$$\Rightarrow \frac{\delta E_{\mathrm{x}}}{\delta V(\boldsymbol{r}'')} = -\frac{1}{2\pi\,\mathrm{i}}\lim_{\tau\to 0^-}\iint\limits_{\mathbb{R}^3\mathbb{R}^3} d^3\boldsymbol{r}d^3\boldsymbol{r}'\int\limits_{-\infty}^{\infty} d\omega\, G_0(\boldsymbol{r}'',\boldsymbol{r}',\omega)V_{\mathrm{x}}(\boldsymbol{r}',\boldsymbol{r})G_0(\boldsymbol{r},\boldsymbol{r}'',\omega)e^{-\mathrm{i}\omega\tau}. \tag{190}$$

Again, as was the case for the Hartree term, in accordance with equations (164) to (167), the expression above (190) can be written in terms of the one electron orbitals as:

$$\frac{\delta E_{\mathrm{x}}}{\delta V(\boldsymbol{r}'')} = \langle\boldsymbol{r}''|\sum_{i\in occ, n\neq i}\frac{|i\rangle\langle i|V_{\mathrm{x}}|n\rangle\langle n| + |n\rangle\langle n|V_{\mathrm{x}}|i\rangle\langle i|}{\epsilon_i-\epsilon_n}|\boldsymbol{r}''\rangle\,. \tag{191}$$

7.1.3 Variation of the kinetic energy E_{kin}

Proceeding with the variation of the kinetic energy δE_{kin},

$$\delta E_{\mathrm{kin}} = -\frac{1}{2}\iint\limits_{\mathbb{R}^3\mathbb{R}^3} d^3\boldsymbol{r}d^3\boldsymbol{r}'\,\delta(\boldsymbol{r}-\boldsymbol{r}')\nabla^2_{\boldsymbol{r}'}\delta n(\boldsymbol{r}'\boldsymbol{r}) \tag{192}$$

and using equation (180) one gets

$$-4\pi\,\mathrm{i}\;\delta E_{\mathrm{kin}} =$$

$$\int\limits_{\mathbb{R}^3} d^3\boldsymbol{r}''\lim_{\tau\to 0^+}\iint\limits_{\mathbb{R}^3\mathbb{R}^3} d^3\boldsymbol{r}d^3\boldsymbol{r}'\,\delta(\boldsymbol{r}-\boldsymbol{r}')\int\limits_{-\infty}^{\infty} d\omega\,\nabla^2_{\boldsymbol{r}'}G_0(\boldsymbol{r}',\boldsymbol{r}'',\omega)G_0(\boldsymbol{r}'',\boldsymbol{r},\omega)e^{\mathrm{i}\omega\tau}\delta V(\boldsymbol{r}'') \tag{193}$$

$$\Rightarrow \frac{\delta E_{\mathrm{kin}}}{\delta V(\boldsymbol{r}'')} = -\frac{1}{4\pi\,\mathrm{i}}\lim_{\tau\to 0^-}\iint\limits_{\mathbb{R}^3\mathbb{R}^3} d^3\boldsymbol{r}d^3\boldsymbol{r}'\int\limits_{-\infty}^{\infty} d\omega\,G_0(\boldsymbol{r}'',\boldsymbol{r},\omega)\delta(\boldsymbol{r}-\boldsymbol{r}')\nabla^2_{\boldsymbol{r}'}G_0(\boldsymbol{r}',\boldsymbol{r}'',\omega)e^{-\mathrm{i}\omega\tau}. \tag{194}$$

7.1.4 Variation of the external energy E_{ext}

Finally δE_{ext} can be calculated as follows

$$\delta E_{\mathrm{ext}} = \left[\frac{\delta E_{\mathrm{ext}}}{\delta V(\boldsymbol{r}'')}\right]_{R_k}\delta V + \sum_k \left[\nabla_{\boldsymbol{R}_k}E_{\mathrm{ext}}\right]_n\cdot\delta\boldsymbol{R}_k \tag{195}$$

where $[\,]_x$ means $x = const.$

$$\left[\frac{\delta E_{\mathrm{ext}}}{\delta V(\boldsymbol{r}'')}\right]_{R_k} = \frac{1}{2\pi\,\mathrm{i}}\lim_{\tau\to 0^+}\sum_k\int\limits_{\mathbb{R}^3} d^3\boldsymbol{r}\int_{-\infty}^{\infty} d\omega\,\frac{G_0(\boldsymbol{r},\boldsymbol{r}'',\omega)G_0(\boldsymbol{r}'',\boldsymbol{r},\omega)}{|\boldsymbol{r}-\boldsymbol{R}_k|}e^{\mathrm{i}\omega\tau} \tag{196}$$

$$\left[\nabla_{\boldsymbol{R}_k}E_{\mathrm{ext}}\right]_n = \int\limits_{\mathbb{R}^3} d^3\boldsymbol{r}\frac{n(\boldsymbol{r})}{|\boldsymbol{r}-\boldsymbol{R}_k|^3}(\boldsymbol{r}-\boldsymbol{R}_k) \tag{197}$$

7.2 Variation of the Random Phase Approximation (RPA) correlation energy $E_{\mathrm{c}}^{\mathrm{RPA}}$ with the Green's function method

The Hartree-Fock method assumes the many-body ground state can be written as a single Slater determinant. This ansatz yields an energy functional that estimates the Coulomb interaction between the electrons via a mean-field ansatz. Additionally the so called exchange term, E_{x}, is included and takes care that two electrons with parallel spin may never occupy the same position eigenstate, or classically spoken may never be at the same position at any time. However, the Hartree-Fock method neglects instantaneous Coulomb interactions between the electrons.

Since the exact ground state will generally not be a single Slater determinant, the Hartree-Fock energy functional gives only an upper bound for the ground state energy. The difference of the Hartree-Fock energy to the exact (non relativistic) ground state energy is called correlation energy, E_c.

$$E_\mathrm{c} = E_\mathrm{HF} - E_\mathrm{exact} \tag{198}$$

Following the arguments above, E_c can be interpreted as the decrease of the ground state energy due to the instantaneous Coulomb interaction described above.

In the RPA, E_c can expressed as follows (see section 3, equation 136):

$$E_\mathrm{c}^\mathrm{RPA} = \frac{1}{4\pi}\int_{-\infty}^{\infty} d\nu\, \mathrm{Tr}\{\ln(1-\chi(\mathrm{i}\,\nu)\,\mathrm{v}) + \chi(\mathrm{i}\,\nu)\,\mathrm{v}\}. \tag{199}$$

Here v is the Coulomb potential and $\chi(i\nu)$ is the independent particle polarizability (= Kohn-Sham response function) in the imaginary frequency domain. The functional $\ln(1-X)$ of an operator X can be defined by the power series

$$\ln(1-X) = -\sum_{n=1}^{\infty}\frac{X^n}{n} \tag{200}$$

Now the change of the energy due to changes in the external potential shall be calculated. $E_\mathrm{c}^\mathrm{RPA}$ is affected by changes of the external potential via the response function $\chi(\mathrm{i}\,\nu)$. The following relations connect χ with the Green's function [26]

$$\tilde{\chi}(\boldsymbol{r},\boldsymbol{r}',\mathrm{i}\,\tau) = -G_0(\boldsymbol{r},\boldsymbol{r}',\mathrm{i}\,\tau)G_0(\boldsymbol{r}',\boldsymbol{r},-\mathrm{i}\,\tau) \tag{201}$$

$$\chi(\mathrm{i}\,\nu) = \int_{-\infty}^{\infty} d\tau\, \tilde{\chi}(\mathrm{i}\,\tau)e^{\mathrm{i}\,\nu\tau} \tag{202}$$

This can be exploited in order to calculate $\delta E_\mathrm{c}^{RPA}$ by following a similar approach as that used to evaluate δE_HF. First the functional derivative of $E_\mathrm{c}^\mathrm{RPA}$ with respect to $\chi(\boldsymbol{r},\boldsymbol{r}',\mathrm{i}\,\nu)$ has to be calculated. Multiplying the result by $\delta\chi(\boldsymbol{r},\boldsymbol{r}',\mathrm{i}\,\nu)$ and integrating over all $\boldsymbol{r}$, $\boldsymbol{r}'$ and ν yields the total change of the correlation energy $\delta E_\mathrm{c}^\mathrm{RPA}$.

$$\delta E_\mathrm{c}^\mathrm{RPA} = \int_{-\infty}^{\infty} d\boldsymbol{r}d\boldsymbol{r}'d\nu \frac{\delta E_\mathrm{c}^\mathrm{RPA}}{\delta\chi(\boldsymbol{r},\boldsymbol{r}',\mathrm{i}\,\nu)}\delta\chi(\boldsymbol{r},\boldsymbol{r}',\mathrm{i}\,\nu) \tag{203}$$

In order to calculate $\frac{\delta E_\mathrm{c}^{RPA}}{\delta\chi}$, it is useful to derive some general expressions for the functional derivative of the trace of an operator. Consider some operator Y with eigenvalues

λ_n^Y and eigenstates $|\phi_n^Y\rangle$ and a function F(), so that

$$\mathrm{F}(Y) = \sum_n \mathrm{F}(\lambda_n^Y)\, |\phi_n^Y\rangle\, \langle\phi_n^Y| \tag{204}$$

Now the differential of the trace of $\mathrm{F}(Y)$ may be calculated as follows:

$$\mathrm{dTr}\{\mathrm{F}(Y)\} = \mathrm{Tr}\{\frac{\mathrm{dF}(Y)}{\mathrm{d}\,Y}\,\mathrm{d}\,Y\}. \tag{205}$$

Since

$$\mathrm{Tr}\{AB\} = \mathrm{Tr}\{BA\}, \tag{206}$$

equation (205) yields the same result, regardless of the order in which the operators occur on the right hand side. However, care must be taken if Y is itself a function of another operator. The simplest non-trivial case is

$$Y = A + XB \tag{207}$$

where A and B are not subject to the variation, then

$$\mathrm{dTr}\{\mathrm{F}(Y)\} = \mathrm{Tr}\{\frac{\mathrm{dF}(Y)}{\mathrm{d}\,Y}\,\mathrm{d}XB\} = \mathrm{Tr}\{\mathrm{d}XB\frac{\mathrm{dF}(Y)}{\mathrm{d}\,Y}\} = \mathrm{Tr}\{B\frac{\mathrm{dF}(Y)}{\mathrm{d}\,Y}\,\mathrm{d}X\}. \tag{208}$$

Now the order of the operators occurring in the trace is important and generally only cyclic permutations are allowed. Note that generally

$$\mathrm{dTr}\{\mathrm{F}(A + BX)\} \neq \mathrm{dTr}\{\mathrm{F}(A + XB)\}. \tag{209}$$

Applying this rules, one obtains

$$\frac{\delta E_{\mathrm{c}}^{\mathrm{RPA}}}{\delta\chi(\boldsymbol{r},\boldsymbol{r}',\mathrm{i}\,\nu)} = \frac{1}{4\pi}\int_{-\infty}^{\infty} d\nu' \frac{\delta \mathrm{Tr}\{\ln(1-\chi(\mathrm{i}\,\nu')\,\mathrm{v}) + \chi(\mathrm{i}\,\nu')\,\mathrm{v}\}}{\delta\chi(\boldsymbol{r},\boldsymbol{r}',\mathrm{i}\,\nu)} \tag{210}$$

$$= \frac{1}{4\pi}\int_{-\infty}^{\infty} d\nu'\, \mathrm{Tr}\{(1-(1-\chi(\mathrm{i}\,\nu')\,\mathrm{v})^{-1}) \frac{\delta\chi(\mathrm{i}\,\nu')}{\delta\chi(\boldsymbol{r},\boldsymbol{r}',\mathrm{i}\,\nu)}\,\mathrm{v}\} \tag{211}$$

$$= \frac{1}{4\pi}\int_{-\infty}^{\infty} d\nu'\, d\boldsymbol{s}\, d\boldsymbol{s}'\, d\boldsymbol{s}''\, \big(1-(1-\chi(\mathrm{i}\,\nu')\,\mathrm{v})^{-1}\big)(\boldsymbol{s},\boldsymbol{s}') \frac{\delta\chi(\boldsymbol{s}',\boldsymbol{s}'',\mathrm{i}\,\nu')}{\delta\chi(\boldsymbol{r},\boldsymbol{r}',\mathrm{i}\,\nu)}\, \mathrm{v}(\boldsymbol{s}'',\boldsymbol{s}) \tag{212}$$

$$= \frac{1}{4\pi}\int_{-\infty}^{\infty} d\nu'\, d\boldsymbol{s}\, d\boldsymbol{s}'\, d\boldsymbol{s}''\, \big(1-(1-\chi(\mathrm{i}\,\nu')\,\mathrm{v})^{-1}\big)(\boldsymbol{s},\boldsymbol{s}')$$

$$\times\, \delta(\boldsymbol{s}'-\boldsymbol{r})\,\delta(\boldsymbol{s}''-\boldsymbol{r}')\,\delta(\nu'-\nu)\, \mathrm{v}(\boldsymbol{s}'',\boldsymbol{s}) \tag{213}$$

$$= \frac{1}{4\pi}\int_{\mathbb{R}^3} ds\, \mathrm{v}(\boldsymbol{r}',\boldsymbol{s})\,\big(1-(1-\chi(\mathrm{i}\,\nu)\,\mathrm{v})^{-1}\big)(\boldsymbol{s},\boldsymbol{r}) \tag{214}$$

and finally

$$\Rightarrow \frac{\delta E_{\mathrm{c}}^{\mathrm{RPA}}}{\delta\chi(\boldsymbol{r},\boldsymbol{r}',\mathrm{i}\,\nu)} = \frac{1}{4\pi}\,\big(\mathrm{v}-\mathrm{v}\,(1-\chi(\mathrm{i}\,\nu)\,\mathrm{v})^{-1}\big)(\boldsymbol{r}',\boldsymbol{r}) \tag{215}$$

$$= -\left[\mathrm{v}\sum_{n=1}^{\infty}(\chi\,\mathrm{v})^n\right](\boldsymbol{r}',\boldsymbol{r}) \tag{216}$$

$$= \left[-W_{\mathrm{c}}(\mathrm{i}\,\nu)\right](\boldsymbol{r}',\boldsymbol{r}) \tag{217}$$

where W_{c} is the correlation part of the screened interaction in the RPA.

The next step is to express $\delta\chi(\boldsymbol{r},\boldsymbol{r}',\mathrm{i}\,\nu)$ from equation (203) in terms of the Greens functions G and the change in the external potential $\delta V(\boldsymbol{r},\boldsymbol{r}')$ by using equation (201) and (202).

$$\delta\chi(\boldsymbol{r},\boldsymbol{r}',\mathrm{i}\,\nu) = \int_{-\infty}^{\infty} d\tau\, \delta\tilde{\chi}(\boldsymbol{r},\boldsymbol{r}',\mathrm{i}\,\tau)\, e^{\mathrm{i}\,\tau\nu} \tag{218}$$

$$= -\int_{-\infty}^{\infty} d\tau e^{\mathrm{i}\,\tau\nu}\{\delta G(\boldsymbol{r},\boldsymbol{r}',\mathrm{i}\,\tau)G_0(\boldsymbol{r}',\boldsymbol{r},-\mathrm{i}\,\tau)$$

$$+ G_0(\boldsymbol{r},\boldsymbol{r}',\mathrm{i}\,\tau)\delta G(\boldsymbol{r}',\boldsymbol{r},-\mathrm{i}\,\tau)\} \tag{219}$$

Since equation (163) is only valid in frequency space, $\delta G(\mathrm{i}\,\tau)$ has to be calculated by a Fourier transform.

$$\delta G(\boldsymbol{r},\boldsymbol{r}',\mathrm{i}\,\tau) = \frac{1}{2\pi}\int_{-\infty}^{\infty} d\nu'\, e^{-\mathrm{i}\,\nu'\tau} \underbrace{\iint_{\mathbb{R}^3\mathbb{R}^3} d\boldsymbol{r}''d\boldsymbol{r}'''G_0(\boldsymbol{r},\boldsymbol{r}'',\mathrm{i}\,\nu')\delta V(\boldsymbol{r}'',\boldsymbol{r}''')G_0(\boldsymbol{r}''',\boldsymbol{r}',\mathrm{i}\,\nu')}_{\delta G(\boldsymbol{r},\boldsymbol{r}',\mathrm{i}\,\nu')} \tag{220}$$

Using this in equation (219) gives

$$\delta\chi(\boldsymbol{r},\boldsymbol{r}',\mathrm{i}\,\nu) = -\frac{1}{2\pi}\int_{-\infty}^{\infty} d\tau\, e^{\mathrm{i}\,\tau\nu}\int_{-\infty}^{\infty} d\nu'\, e^{-\mathrm{i}\,\nu'\tau}\big\{\delta G(\boldsymbol{r},\boldsymbol{r}',\mathrm{i}\,\nu')\, G_0(\boldsymbol{r}',\boldsymbol{r},-\mathrm{i}\,\tau)+$$

$$+G_0(\boldsymbol{r},\boldsymbol{r}',\mathrm{i}\,\tau)\,\delta G(\boldsymbol{r}',\boldsymbol{r},-\mathrm{i}\,\nu')\big\}. \tag{221}$$

The expression for $\delta E_{\mathrm{c}}^{\mathrm{RPA}}$ by just inserting the results from equation (215) and (221) into equation (203) is rather long. For the sake of clarity, some of the terms involved in simplifying $\delta E_{\mathrm{c}}^{\mathrm{RPA}}$ are first written out explicitly as definitions.

$$\mathcal{F}_\nu[f(\mathrm{i}\,\nu)](\mathrm{i}\,\tau) \equiv f(\mathrm{i}\,\tau) \tag{222}$$

The tilde sign ($\tilde{f}$) is omitted, the Fourier transform is usually indicated implicitly by the variable.

$$G_0^-(\boldsymbol{r},\boldsymbol{r}',\mathrm{i}\,\nu) \equiv G_0(\boldsymbol{r},\boldsymbol{r}',-\mathrm{i}\,\nu) \tag{223}$$

$$G_0^T(\boldsymbol{r},\boldsymbol{r}',\mathrm{i}\,\nu) \equiv G_0(\boldsymbol{r}',\boldsymbol{r},\mathrm{i}\,\nu) \tag{224}$$

While the upper index "-" indicates a sign change in the time or frequency variable, the upper index "T" shall denote a interchange of the spatial variables $\boldsymbol{r} \leftrightarrow \boldsymbol{r}'$, or the

momentum variables. Further the point wise multiplication is denominated by $\odot$, e.g.

$$\left(W_{\mathrm{c}} \odot G_0\right)(\boldsymbol{r}, \boldsymbol{r}', \mathrm{i}\,\tau) \equiv W_{\mathrm{c}}(\boldsymbol{r}, \boldsymbol{r}', \mathrm{i}\,\tau) G_0(\boldsymbol{r}, \boldsymbol{r}', \mathrm{i}\,\tau) \tag{225}$$

With the results from equation (215) and (221) and the definitions above, $\delta E_{\mathrm{c}}^{\mathrm{RPA}}$ can be written in a compact form by rearranging some terms and performing the integrals.

$$\begin{aligned}
\delta E_{\mathrm{c}}^{\mathrm{RPA}} &= -\int_{-\infty}^{\infty} d\boldsymbol{r} d\boldsymbol{r}' d\nu \frac{\delta E_{\mathrm{c}}^{RPA}}{\delta \chi(\boldsymbol{r}, \boldsymbol{r}', \mathrm{i}\,\nu)} \frac{1}{2\pi} \int_{-\infty}^{\infty} d\nu' d\tau\, e^{i\nu\tau}\, e^{-\mathrm{i}\,\nu'\tau} \\
&\quad \times \left\{ \delta G(\boldsymbol{r}, \boldsymbol{r}', \mathrm{i}\,\nu')\, G_0(\boldsymbol{r}', \boldsymbol{r}, -\mathrm{i}\,\tau) + G_0(\boldsymbol{r}, \boldsymbol{r}', \mathrm{i}\,\tau)\, \delta G(\boldsymbol{r}', \boldsymbol{r}, -\mathrm{i}\,\nu') \right\} \qquad (226) \\
&= -\int_{-\infty}^{\infty} d\boldsymbol{r} d\boldsymbol{r}' d\nu' \Big\{ \delta G(\boldsymbol{r}, \boldsymbol{r}', \mathrm{i}\,\nu') \int_{-\infty}^{\infty} d\tau\, e^{-\mathrm{i}\,\nu'\tau} \frac{\delta E_{\mathrm{c}}^{RPA}}{\delta \chi(\boldsymbol{r}, \boldsymbol{r}', -\mathrm{i}\,\tau)} G_0(\boldsymbol{r}', \boldsymbol{r}, -\mathrm{i}\,\tau) \\
&\quad + \delta G(\boldsymbol{r}', \boldsymbol{r}, -\mathrm{i}\,\nu') \int_{-\infty}^{\infty} d\tau\, e^{-\mathrm{i}\,\nu'\tau} \frac{\delta E_{\mathrm{c}}^{RPA}}{\delta \chi(\boldsymbol{r}, \boldsymbol{r}', -\mathrm{i}\,\tau)} G_0(\boldsymbol{r}, \boldsymbol{r}', \mathrm{i}\,\tau) \Big\} \qquad (227) \\
&= \int_{-\infty}^{\infty} d\boldsymbol{r} d\boldsymbol{r}' d\nu' \Big\{ \delta G(\boldsymbol{r}, \boldsymbol{r}', \mathrm{i}\,\nu') \int_{-\infty}^{\infty} d\tau\, e^{-\mathrm{i}\,\nu'\tau} W_{\mathrm{c}}(\boldsymbol{r}', \boldsymbol{r}, -\mathrm{i}\,\tau) G_0(\boldsymbol{r}', \boldsymbol{r}, -\mathrm{i}\,\tau) \\
&\quad + \delta G(\boldsymbol{r}', \boldsymbol{r}, -\mathrm{i}\,\nu') \int_{-\infty}^{\infty} d\tau\, e^{-\mathrm{i}\,\nu'\tau} W_{\mathrm{c}}(\boldsymbol{r}', \boldsymbol{r}, -\mathrm{i}\,\tau) G_0(\boldsymbol{r}, \boldsymbol{r}', \mathrm{i}\,\tau) \Big\} \qquad (228) \\
&= \int_{-\infty}^{\infty} d\boldsymbol{r} d\boldsymbol{r}' d\nu' \Big\{ \delta G(\boldsymbol{r}, \boldsymbol{r}', \mathrm{i}\,\nu') \mathcal{F}_\tau \left[W_{\mathrm{c}} \odot G_0 \right](\boldsymbol{r}', \boldsymbol{r}, \mathrm{i}\,\nu') \\
&\quad + \delta G(\boldsymbol{r}', \boldsymbol{r}, -\mathrm{i}\,\nu') \mathcal{F}_\tau \left[W_{\mathrm{c}}^{T-} \odot G_0 \right](\boldsymbol{r}, \boldsymbol{r}', -\mathrm{i}\,\nu') \Big\} \qquad (229)
\end{aligned}$$

Note that for $\mathcal{F}_\tau \left[W_{\mathrm{c}} \odot G_0 \right](\boldsymbol{r}', \boldsymbol{r}, \mathrm{i}\,\nu')$ the point wise multiplication has to be performed in the imaginary time domain prior to the Fourier transformation to imaginary frequency.

Using equation(163) for δG, finally

$$\delta E_{\mathrm{c}}^{\mathrm{RPA}} = \int_{-\infty}^{\infty} d\boldsymbol{r}'' d\boldsymbol{r}''' \frac{\delta E_{\mathrm{c}}^{\mathrm{RPA}}}{\delta V(\boldsymbol{r}'', \boldsymbol{r}''')} \delta V(\boldsymbol{r}'', \boldsymbol{r}''') = \mathrm{Tr}\left\{ \frac{\delta E_{\mathrm{c}}^{\mathrm{RPA}}}{\delta V}\, \delta V \right\}, \tag{230}$$

where

$$\frac{\delta E_{\mathrm{c}}^{RPA}}{\delta V(\boldsymbol{r}'',\boldsymbol{r}''')} = \int_{-\infty}^{\infty} d\boldsymbol{r}d\boldsymbol{r}'d\nu \big\{ G_0(\boldsymbol{r}''',\boldsymbol{r}',\mathrm{i}\,\nu)\mathcal{F}_\tau\left[W_{\mathrm{c}} \odot G_0\right](\boldsymbol{r}',\boldsymbol{r},\mathrm{i}\,\nu)G_0(\boldsymbol{r},\boldsymbol{r}'',\mathrm{i}\,\nu)$$

$$+ G_0(\boldsymbol{r}''',\boldsymbol{r}',-\mathrm{i}\,\nu)\mathcal{F}_\tau\left[W_{\mathrm{c}}^{T-} \odot G_0\right](\boldsymbol{r}',\boldsymbol{r},-\mathrm{i}\,\nu)G_0(\boldsymbol{r},\boldsymbol{r}'',-\mathrm{i}\,\nu)\big\} \quad (231)$$

$$= \langle \boldsymbol{r}''' | \int_{-\infty}^{\infty} d\nu \left(G_0\, \mathcal{F}_\tau\left[W_{\mathrm{c}} \odot G_0\right] G_0\right)(\mathrm{i}\,\nu) + \left(G_0\, \mathcal{F}_\tau\left[W_{\mathrm{c}}^{T-} \odot G_0\right] G_0\right)(-\mathrm{i}\,\nu) | \boldsymbol{r}'' \rangle \quad (232)$$

$$= \langle \boldsymbol{r}''' | \frac{\delta E_{\mathrm{c}}^{RPA}}{\delta V} | \boldsymbol{r}'' \rangle \,. \quad (233)$$

From equation (231) to (232), we switched to a more compact operator notation.

8 Feynman diagramtic representation of the energy Variations

In this section, the expressions for the variation of the Hartree, exchange and correlation energy will be translated into Feynman diagrams to provide a good overview and to give a more compact presentation of the results. For this reason the expressions will first be transformed to the time domain and then be translated into diagrams. The rules for the translation will not be discussed, but can be found in references [7] and [16]. However a very short description shall be given at this point.

The Green's function $G_0(\boldsymbol{r}', \boldsymbol{r}, t' - t)$ is represented by a single line with an arrow. The line connects the coordinate point $(\boldsymbol{r}', t')$ with $(\boldsymbol{r}, t)$ and the arrow points in the direction of increasing time or $(t' - t) > 0$ in the opposite direction for $(t' - t) \leq 0$. In this theses, it is implicitly assumed that the time coordinate is on the vertical axis while spatial coordinates are on the horizontal axis.

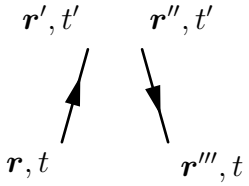

The interaction $V(\boldsymbol{r}, \boldsymbol{r}')$, in our case the Coulomb interaction v, between two particles is represented by a single wiggly line.

In this framework, we write the correlation part of the screened interaction in the RPA W_c as a double wiggly line which is written in terms of the above diagrams as

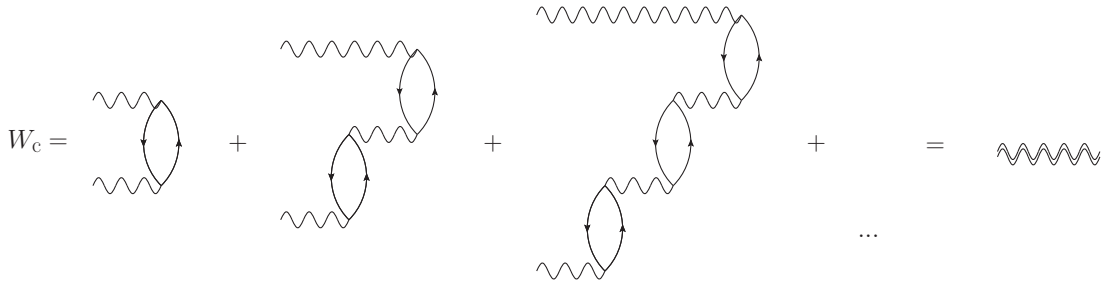

Finally note that it is integrated over all intermediate times and frequencies.

8.1 Hartree term

First the results from section 7.1.1 are transformed into the time domain.

$$\frac{\delta E_{\mathrm{H}}}{\delta V(\boldsymbol{r})} = \frac{1}{2\pi\,\mathrm{i}} \lim_{\tau\to 0^-} \int\limits_{\mathbb{R}^3} d^3\boldsymbol{r}' \int\limits_{-\infty}^{\infty} d\omega\, G_0(\boldsymbol{r},\boldsymbol{r}',\omega) \int\limits_{\mathbb{R}^3} d^3\boldsymbol{r}'' \frac{n(\boldsymbol{r}'')}{|\boldsymbol{r}'-\boldsymbol{r}''|} G_0(\boldsymbol{r}',\boldsymbol{r},\omega) e^{-\,\mathrm{i}\,\omega\tau} \tag{234}$$

$$= -\frac{1}{2\pi} \lim_{\tau\to 0^-} \int d^3\boldsymbol{r}' d^3\boldsymbol{r}'' d\omega\, dt\, dt' G_0(\boldsymbol{r},\boldsymbol{r}',t)\, \mathrm{v}(\boldsymbol{r}',\boldsymbol{r}'') G_0(\boldsymbol{r}'',\boldsymbol{r}'',0^-) G_0(\boldsymbol{r}',\boldsymbol{r},t') e^{-\,\mathrm{i}\,\omega(\tau-t-t')} \tag{235}$$

$$= -\int d^3\boldsymbol{r}' d^3\boldsymbol{r}''\, dt\, dt'\, G_0(\boldsymbol{r}',\boldsymbol{r},t') G_0(\boldsymbol{r},\boldsymbol{r}',t)\, \mathrm{v}(\boldsymbol{r}',\boldsymbol{r}'') G_0(\boldsymbol{r}'',\boldsymbol{r}'',0^-) \delta(t+t') \tag{236}$$

$$= -\int d^3\boldsymbol{r} d^3\boldsymbol{r}'\, dt\, G_0(\boldsymbol{r}',\boldsymbol{r},-t) G_0(\boldsymbol{r},\boldsymbol{r}',t)\, \mathrm{v}(\boldsymbol{r}',\boldsymbol{r}'') G_0(\boldsymbol{r}'',\boldsymbol{r}'',0^-) \tag{237}$$

From equation (234) to (235), we used the representation of the density with respect to the Green's function, see equation (161) and wrote the Green's functions in frequency space as explicit Fourier transforms from the time domain. The ω-integration in equation (236) yields $\delta(t+t')$. Expression (237) can now easily be translated to the diagram:

$\frac{\delta E_{\mathrm{H}}}{\delta V(r)} =$

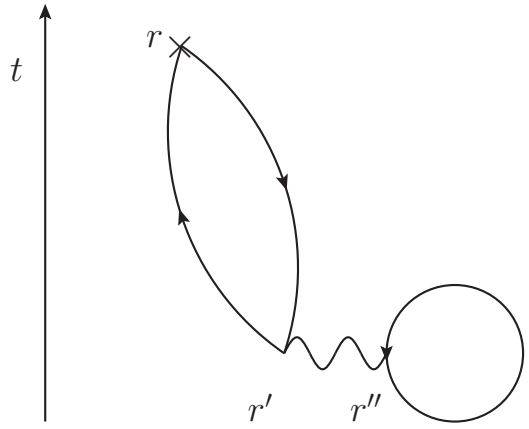

(238)

The $\times$-symbol indicates that $\boldsymbol{r}$ is not subject to the integration.

8.2 Exchange term

In a similar manner the results from section 7.1.2 are transformed into the time domain.

$$\frac{\delta E_{\mathrm{H}}}{\delta V(\boldsymbol{r})} = \frac{1}{2\pi\,\mathrm{i}} \lim_{\tau\to 0^-} \int\limits_{\mathbb{R}^3} d^3\boldsymbol{r}' \int\limits_{-\infty}^{\infty} d\omega\, G_0(\boldsymbol{r},\boldsymbol{r}'',\omega) \int\limits_{\mathbb{R}^3} d^3\boldsymbol{r}'' \frac{n(\boldsymbol{r}'',\boldsymbol{r}')}{|\boldsymbol{r}'-\boldsymbol{r}''|} G_0(\boldsymbol{r}',\boldsymbol{r},\omega) e^{-\,\mathrm{i}\,\omega\tau} \tag{239}$$

$$= -\frac{1}{2\pi} \lim_{\tau\to 0^-} \int d^3\boldsymbol{r}' d^3\boldsymbol{r}'' d\omega\, dt\, dt' G_0(\boldsymbol{r},\boldsymbol{r}'',t)\, \mathrm{v}(\boldsymbol{r}',\boldsymbol{r}'') G_0(\boldsymbol{r}'',\boldsymbol{r}',0^-) G_0(\boldsymbol{r}',\boldsymbol{r},t') e^{-\,\mathrm{i}\,\omega(\tau-t-t')} \tag{240}$$

$$= -\int d^3\boldsymbol{r}' d^3\boldsymbol{r}''\, dt\, dt'\, G_0(\boldsymbol{r},\boldsymbol{r}'',t)\, \mathrm{v}(\boldsymbol{r}',\boldsymbol{r}'') G_0(\boldsymbol{r}'',\boldsymbol{r}',0^-) G_0(\boldsymbol{r}',\boldsymbol{r},t') \delta(t+t') \tag{241}$$

$$= -\int d^3\boldsymbol{r}' d^3\boldsymbol{r}''\, dt\, G_0(\boldsymbol{r},\boldsymbol{r}'',t)\, \mathrm{v}(\boldsymbol{r}',\boldsymbol{r}'') G_0(\boldsymbol{r}'',\boldsymbol{r}',0^-) G_0(\boldsymbol{r}',\boldsymbol{r},-t) \tag{242}$$

This result is translated into the diagram as follows:

$\frac{\delta E_{\mathrm{x}}}{\delta V(r)} =$

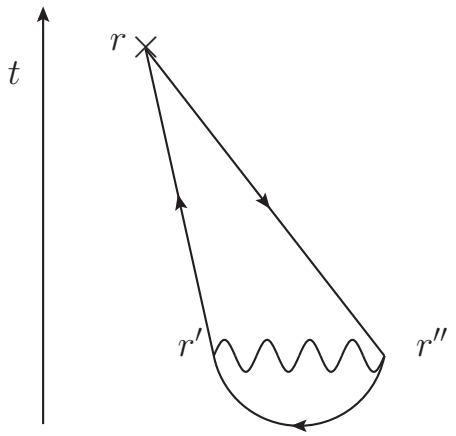

(243)

8.3 RPA-correlation term

In order to translate the functional derivative of the RPA-correlation energy with respect to the KS-potential into diagrams we start from equation (231), but only consider the first term in the integral. The second term will be treated separately afterwards.

$$\int_{-\infty}^{\infty} d\boldsymbol{r}' d\boldsymbol{r}'' d\nu \, d\tau \, e^{i\tau\nu} G_0(\boldsymbol{r}, \boldsymbol{r}'', \mathrm{i}\,\nu) W_\mathrm{c}(\boldsymbol{r}'', \boldsymbol{r}', \mathrm{i}\,\tau) G_0(\boldsymbol{r}'', \boldsymbol{r}', \mathrm{i}\,\tau) G_0(\boldsymbol{r}', \boldsymbol{r}, \mathrm{i}\,\nu) = \tag{244}$$

$$\int_{-\infty}^{\infty} d\boldsymbol{r}' d\boldsymbol{r}'' d\nu \, d\tau \, d\tau' \, d\tau'' \, e^{i\nu(\tau+\tau'+\tau'')} \times$$

$$\times G_0(\boldsymbol{r}, \boldsymbol{r}'', \mathrm{i}\,\tau') W_\mathrm{c}(\boldsymbol{r}'', \boldsymbol{r}', \mathrm{i}\,\tau) G_0(\boldsymbol{r}'', \boldsymbol{r}', \mathrm{i}\,\tau) G_0(\boldsymbol{r}', \boldsymbol{r}, \mathrm{i}\,\tau'') = \tag{245}$$

$$\int_{-\infty}^{\infty} d\boldsymbol{r}' d\boldsymbol{r}'' d\tau \, d\tau' \, d\tau'' \, \delta(\tau + \tau' + \tau'') \times$$

$$\times G_0(\boldsymbol{r}, \boldsymbol{r}'', \mathrm{i}\,\tau') W_\mathrm{c}(\boldsymbol{r}'', \boldsymbol{r}', \mathrm{i}\,\tau) G_0(\boldsymbol{r}'', \boldsymbol{r}', \mathrm{i}\,\tau) G_0(\boldsymbol{r}', \boldsymbol{r}, \mathrm{i}\,\tau'') = \tag{246}$$

$$\int_{-\infty}^{\infty} d\boldsymbol{r}' d\boldsymbol{r}'' d\tau \, d\tau' \, G_0(\boldsymbol{r}, \boldsymbol{r}'', \mathrm{i}\,\tau') W_\mathrm{c}(\boldsymbol{r}'', \boldsymbol{r}', \mathrm{i}\,\tau) G_0(\boldsymbol{r}'', \boldsymbol{r}', \mathrm{i}\,\tau) G_0(\boldsymbol{r}', \boldsymbol{r}, -\mathrm{i}(\tau + \tau')) \tag{247}$$

This yields the following diagram:

$$\frac{\delta E_\mathrm{C}^\mathrm{RPA}}{\delta V(r)} =$$

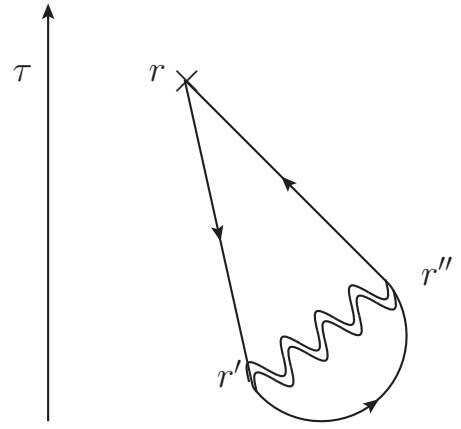

(248)

For the second term from equation (231) one can proceed similarly, yielding topologically the same diagram.

$$\int_{-\infty}^{\infty} d\boldsymbol{r}' d\boldsymbol{r}'' d\nu \, d\tau \, e^{-i\tau\nu} G_0(\boldsymbol{r}, \boldsymbol{r}'', -\mathrm{i}\,\nu) W_\mathrm{c}(\boldsymbol{r}', \boldsymbol{r}'', -\mathrm{i}\,\tau) G_0(\boldsymbol{r}'', \boldsymbol{r}', \mathrm{i}\,\tau) G_0(\boldsymbol{r}', \boldsymbol{r}, -\mathrm{i}\,\nu) = \tag{249}$$

$$\int_{-\infty}^{\infty} d\boldsymbol{r}' d\boldsymbol{r}'' d\tau \, d\tau' \, G_0(\boldsymbol{r}, \boldsymbol{r}'', \mathrm{i}\,\tau') W_\mathrm{c}(\boldsymbol{r}', \boldsymbol{r}'', -\mathrm{i}\,\tau) G_0(\boldsymbol{r}'', \boldsymbol{r}', \mathrm{i}\,\tau) G_0(\boldsymbol{r}', \boldsymbol{r}, -\mathrm{i}(\tau + \tau')) \tag{250}$$

$\frac{\delta E_\mathrm{C}^\mathrm{RPA}}{\delta V(r)} =$

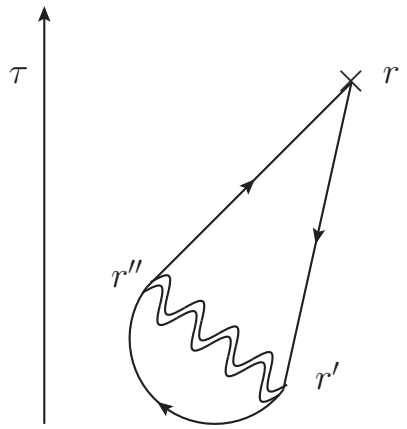

(251)

9 Conclusion

Analytical expressions for the functional derivatives of different energy contributions were derived in this work, employing the Green's function method. This was done for the Hartree-, exchange-, RPA-correlation- and kinetic energy as well as for the energy due to the electrostatic field of the cores. The expressions for $\frac{\delta E_{\mathrm{H}}}{\delta V}$, $\frac{\delta E_{\mathrm{x}}}{\delta V}$ and $\frac{\delta E_{\mathrm{c}}^{\mathrm{RPA}}}{\delta V}$ have all in common that there are two Green's functions to be integrated over, which themselves are connected via an effective interaction, namely V_{H}, V_{x} and W_{c}. This can be seen easily from the diagrammatic expressions (238), (243), (248) and (251). The functional derivatives which were derived in this thesis offer a promising prospect to efficiently compute forces in the RPA, by employing equation (168).

However, there is a lot of work to be done until the method can be implemented fully. First and foremost, the programming in order to embed the method into existing routines will be challenging. Fortunately the functional derivatives contain terms that are in principle available in the latest `VASP` version, hence it will be helpful to exploit the existing routines. Another point is that for the method to work, it has to be combined with an efficient way to compute the derivative of the Kohn-Sham potential with respect to atomic positions. To implement this is also subject of future work.

Once those rather technical issues can be overcome, the method has to be evaluated and tested. The testing can be done against DFT calculations on the one hand, but what is more important is to test against other RPA calculations. One way would be to calculate forces directly with finite steps, however this can be done only at very high computational effort.

If the method turns out to be valid and efficient, there are many applications such as determining vibrational properties and conducting relaxations. There is also an incentive to gather data to provide training test sets for neural networks. That way forces on atom cores can be calculated with the same precision as for the RPA, but without doing the actual RPA calculations for the investigated system.

The simulations on bimolecular complexes, discussed in section 4, revealed that the RPA method showed the desired $\frac{1}{V^2}$-behaviour for large unit cell volumes V. According to the literature values, the RPA results improved in comparison to the DFT results. Future work would include the other complexes of the S-22 test set, as well as simulations with a greater number of different unit cell volumes.

References

[1] Merzuk Kaltak, Jiří Klimeš, and Georg Kresse. "Low scaling algorithms for the random phase approximation: Imaginary time and laplace transformations". In: *Journal of Chemical Theory and Computation* 10.6 (June 2014), pp. 2498–2507. ISSN: 15499626. DOI: 10.1021/ct5001268.

[2] Asbjörn M. Burow et al. "Analytical first-order molecular properties and forces within the adiabatic connection random phase approximation". In: *Journal of Chemical Theory and Computation* 10.1 (2014), pp. 180–194. ISSN: 15499618. DOI: 10.1021/ct4008553.

[3] Stefan Grimme. "Semiempirical GGA-type density functional constructed with a long-range dispersion correction". In: *Journal of Computational Chemistry* 27.15 (2006), pp. 1787–1799. ISSN: 01928651. DOI: 10.1002/jcc.20495.

[4] Wuming Zhu et al. "Range-separated density-functional theory with random phase approximation applied to noncovalent intermolecular interactions". In: 1 (Apr. 2014), pp. 1–9. DOI: 10.1063/1.3431616.

[5] P. Hohenberg and W. Kohn. "The Inhomogeneous Electron Gas". In: *Phys. Rev.* 136 (1964), B864. ISSN: 01631829. DOI: 10.1103/PhysRevB.7.1912.

[6] W Kohn and L J Sham. "Self-consistent equations including exchange and correlation effects". In: *Physical Review* 140.4A (1965). ISSN: 0031899X. DOI: 10.1103/PhysRev.140.A1133.

[7] Alexander L Fetter and John Dirk Walecka. *Quantum Theory of Many-Particle Systems*. Courier Corporation, 2003. ISBN: 0-486-42827-3.

[8] D. M. Ceperley and B. J. Alder. "Ground state of the electron gas by a stochastic method". In: *Physical Review Letters* 45.7 (1980), pp. 566–569. ISSN: 00319007. DOI: 10.1103/PhysRevLett.45.566.

[9] John P. Perdew and Yue Wang. "Accurate and simple analytic representation of the electron-gas correlation energy". In: *Physical Review B* 45.23 (1992), pp. 13244–13249. ISSN: 01631829. DOI: 10.1103/PhysRevB.45.13244.

[10] John P. Perdew, Kieron Burke, and Matthias Ernzerhof. *Generalized Gradient Approximation Made Simple*. 1996. DOI: 10.1103/PhysRevLett.77.3865.

[11] Aron J Cohen, Paula Mori-Sánchez, and Weitao Yang. "Insights into current limitations of density functional theory." In: *Science (New York, N.Y.)* 321.5890 (2008), pp. 792–794. ISSN: 1095-9203. DOI: 10.1126/science.1158722.

[12] D.C. Langreth and J.P. Perdew. *The exchange-correlation energy of a metallic surface*. 1975. DOI: 10.1016/0038-1098(75)90618-3.

[13] O. Gunnarsson and B. I. Lundqvist. "Exchange and correlation in atoms, molecules, and solids by the spin-density-functional formalism". In: *Physical Review B* 13.10 (1976), pp. 4274–4298. ISSN: 01631829. DOI: 10.1103/PhysRevB.13.4274.

[14] David Langreth and John Perdew. "Exchange-correlation energy of a metallic surface: Wave-vector analysis". In: *Physical Review B* 15.6 (1977), pp. 2884–2901. ISSN: 0556-2805. DOI: 10.1103/PhysRevB.15.2884.

[15] Herbert B. Callen and Theodore a. Welton. "Irreversibility and generalized noise". In: *Physical Review* 83.1 (1951), pp. 34–40. ISSN: 0031899X. DOI: 10.1103/PhysRev.83.34.

[16] Richard D Mattuck. *A Guide to Feynman Diagrams in the Many-Body Problem*. 2. Aufl. Courier Corporation, 1992. ISBN: 0-486-67047-3.

[17] K. Yabana et al. "Real-time, real-space implementation of the linear response time-dependent density-functional theory". In: *Physica Status Solidi (B) Basic Research*. Vol. 243. 5. 2006, pp. 1121–1138. ISBN: 0370-1972. DOI: 10.1002/pssb.200642005.

[18] Mark S. Hybertsen and Steven G. Louie. "Ab initio static dielectric matrices from the density-functional approach. I. Formulation and application to semiconductors and insulators". In: *Physical Review B* 35.11 (1987), pp. 5585–5601. ISSN: 01631829. DOI: 10.1103/PhysRevB.35.5585.

[19] Petr Jurecka et al. *S22 - benchmark noncovalent complexes*. Mar. 2015. URL: http://www.begdb.com/index.php?action=oneDataset&id=4&state=show&order=ASC&by=name_m&method=.

[20] Petr Jurecka et al. "Benchmark database of accurate (MP2 and CCSD(T) complete basis set limit) interaction energies of small model complexes, DNA base pairs, and amino acid pairs." In: *Physical chemistry chemical physics : PCCP* 8.17 (2006), pp. 1985–1993. ISSN: 1463-9076. DOI: 10.1039/b600027d.

[21] Jan Řezáč et al. *Quantum Chemical Benchmark Energy and Geometry Database for Molecular Clusters and Complex Molecular Systems (www.begdb.com): A Users Manual and Examples*. 2008. DOI: 10.1135/cccc20081261.

[22] *VASP Wiki*. Mar. 2015. URL: http://cms.mpi.univie.ac.at/wiki/index.php/Main_page.

[23] Jürgen Furthmüller Georg Kresse Martijn Marsman. *VASP the GUIDE*. Mar. 2015. URL: http://cms.mpi.univie.ac.at/vasp/vasp/.

[24] Judith Harl and Georg Kresse. "Cohesive energy curves for noble gas solids calculated by adiabatic connection fluctuation-dissipation theory". In: *Physical Review B - Condensed Matter and Materials Physics* 77.4 (2008), pp. 1–8. ISSN: 10980121. DOI: 10.1103/PhysRevB.77.045136.

[25] Judith Harl, Laurids Schimka, and Georg Kresse. "Assessing the quality of the random phase approximation for lattice constants and atomization energies of solids". In: *Physical Review B* 81.11 (Mar. 2010), p. 115126. ISSN: 1098-0121. DOI: 10.1103/PhysRevB.81.115126.

[26] Lars Hedin. "New method for calculating the one-particle Green's function with application to the electron-gas problem". In: *Physical Review* 139 (1965). ISSN: 0031899X. DOI: 10.1103/PhysRev.139.A796.

Curriculum Vitae

EDUCATION AND TRAINING

01.10.2013 - today	Master of Science *expected to graduate in June 2015* ▪ Physics University of Vienna Universitätsring 1 1010 Vienna Austria
01.10.2011 – 17.09.2013	Bachelor of Science *graduated with distinction* ▪ Physics University of Vienna Universitätsring 1 1010 Vienna Austria
01.09.2010 – 30.06.2011	Bachelor of Science *graduated with distinction* ▪ Medicinal Chemistry and Pharmaceutical Sciences Dublin Institute of Technology Kevin Street Dublin 7 Irland
01.09.2010 – 30.06.2011	VET Diploma *graduated with distinction* ▪ Biochemistry, Biotechnology and Genetic Engineering Höhere Bundes- Lehr- und Versuchsanstalt für chemische Industrie (College of Chemistry) Rosensteingasse 79 1170 Vienna Austria

WORK EXPERIENCE

July to August 2012 — internship
Erste Group Bank AG
- VBA programming for process optimisation

Banking

July 2008 — internship
Technical University of Vienna
- DNA-Extraction, PCR, Electrophoreses, Biolog® Microarrays

Research in Biotechnology

July 2006 — internship
OMV-Refinery Schwechat
- Quality control and chemical analysis of effluents

Petroleum industry

July 2005 — internship
Rembrandtin Lack GmbH
- Quality control and chemical analysis of lacquers

Lacquer industry

ADDITIONAL INFORMATION

Honours and awards
- Best overall performance and best bachelor thesis in final year of the BSc Medicinal Chemistry and Pharmaceutical Sciences 2011 at Dublin Institute of Technology
- Performance scholarships gained in the academic years 2011/12, 2012/13 and 2013/14 for my studies at the University of Vienna

Date _____ Signature _____